# Disruption of the blood-brain barrier and its close environment following adult exposure to low doses of di(2-ethylhexyl)phthalate alone or in an environmental phthalate mixture in male mice

Delnia Ahmadpour, Sakina Mhaouty-Kodja, Valérie Grange-Messent

# Title

Disruption of the blood-brain barrier and its close environment following adult exposure to low doses of di(2-ethylhexyl)phthalate alone or in an environmental phthalate mixture in male mice


## Author names and affiliations:

Delnia Ahmadpour, Sakina Mhaouty-Kodja and Valérie Grange-Messent*

Sorbonne Université, CNRS, INSERM, Neuroscience Paris-Seine, Institut de Biologie Paris-Seine, 75005 Paris, France

## *Corresponding author

Valérie Grange-Messent

Sorbonne Université, INSERM U1130, CNRS UMR 8246, Neuroscience Paris Seine, Institut de Biologie Paris-Seine, 7 quai St Bernard, 75005, Paris, France.

Tel: +33 1 44 27 36 57

Fax: +33 1 44 27 25 08

e.mail: valerie.messent@sorbonne-universite.fr



## Abstract

We have previously shown that adult male mice exposure to low doses of di(2-ethylhexyl)phthalate (DEHP) alters neural function and behaviour. Whether such exposure also affects the integrity and function of the blood-brain barrier (BBB) remained to be explored. The impact of adult exposure to low doses of DEHP alone or in an environmental phthalate mixture on the BBB integrity and surrounding parenchyma was studied in male

mice. Two-month-old C57BL/6J males were orally exposed for 6 weeks to DEHP alone (0.5, and 50 µg/kg/day) or to DEHP (5 µg/kg/day) in an environmental phthalate mixture. BBB permeability, glial activation and neuroinflammation were investigated in the hypothalamic medial preoptic area (mPOA) and hippocampus involved, respectively on the reproductive and cognitive functions. Exposure to DEHP alone or in a phthalate mixture increased BBB permeability and affected the endothelial accessory tight junction protein zona occludens-1 and caveolae protein Cav-1 in the mPOA and the hippocampal CA1 and CA3 areas. This was associated with an inflammatory profile including astrocyte activation accompanied by enhanced expression of inducible nitric oxide synthase in the mPOA, and a microglial activation in the mPOA and the hippocampal CA1 and CA3 areas. The protein levels of the inflammatory molecule cyclooxygenase-2 were increased in activated microglial cells of the exposed mPOA. None of the major effects induced by DEHP alone or in a mixture was detected in the hippocampal dendate gyrus. The data highlight that environmental exposure to endocrine disruptors such as phthalates, could represent a risk factor for the cerebrovascular function.

## Keywords

Blood–brain barrier, Endocrine disruptors, Phthalates

# 1. Introduction

Phthalates are chemical compounds found in plasticizers and solvents (Kabir et al., 2015) and are among the most frequently detected organic pollutants in the environment. Di-2-ethylhexyl phthalate (DEHP), the most commonly detected phthalate, is widely used to add flexibility to high-molecular-weight polymers used in the manufacture of polyvinyl chloride plastic and is therefore found in containers for the storage of food and beverages. DEHP was also classified by the EU in 2000 as a priority substance “presenting a significant risk to or via the aquatic environment” in the Water Framework Directive 2000/60/EC, which was updated in 2008 and 2013 (Directive 2013/39/EU of the European Parliament and of the Council of 12 August 2013). In addition to DEHP, other phthalates including diethyl phthalate (DEP), dibutyl phthalate (DBP), butyl benzyl phthalate (BBP), and diisobutyl phthalate (DiBP) are also detected in the environment worldwide (Gao and Wen, 2016).

The majority of the *in vivo* studies addressing the effects of phthalate exposure on the nervous system have focused on the effects of perinatal exposure. Furthermore, the effects of exposure to phthalates at low doses during adulthood are still largely under-explored. Our recent study revealed that chronic exposure during adulthood to DEHP at the tolerable daily intake dose (TDI) of 50 µg/kg/day (European Food Safety Authority (EFSA) 2005, 2019) or to a 10-fold lower dose (5 µg/kg/day), close to environmental exposure, disrupts the emission of courtship vocalizations and therefore the initiation of mating in male mice (Dombret et al., 2017). This behavioural alteration was not due to modifications of circulating testosterone levels and/or the integrity of the hypothalamic–pituitary–gonadal axis. It was instead associated with down-regulation of the androgen receptor (AR) in the hypothalamic medial preoptic area (mPOA), the main cerebral area involved in the expression of male sexual behaviour (Dombret et al., 2017). The neural AR plays an important role in the expression of male sexual behaviour (Raskin et al., 2009) and also in the modulation of hippocampal functions as shown by the impaired temporal order memory in mice lacking the neural *AR* (Picot et al., 2016). The male hippocampus does indeed exhibit high sensitivity to androgens

and can thus be targeted by compounds exhibiting anti-androgenic activities. In this context, a previous study showed that prenatal or perinatal exposure to DEHP at 200 µg/kg/d or 10 to 200 mg/kg/d impaired spatial memory and induced anxiety- and depressive-like behaviour in adult male mice, and that these effects were associated with AR down-regulation in the hippocampus (Barakat et al., 2018; Xu et al., 2015).

In the brain, including the hypothalamus and hippocampus, the blood-brain barrier (BBB) present at the level of the cerebral capillary protects cerebral regions from the toxicity of circulating xenobiotics and pathogens thereby providing cerebral homeostasis (Weiss et al., 2009). The BBB is formed by endothelial cells (ECs) which are themselves sealed by tight junctions (TJs) and adherens junctions (Abbott et al., 2010; Weiss et al., 2009), thus limiting the paracellular diffusion of substances. The BBB also provides a gate-like function for substance delivery to brain cells by limiting trans-cellular diffusion via selective carrier-mediated transport systems (Abbott et al., 2010). An extremely low rate of transendothelial vesicular transport also integrates the transcellular pathway to minimize the uptake of substances from blood to brain parenchyma (Villaseñor et al., 2019). Among the different categories of vesicular transport, caveolae appears to be the major element responsible for transcytosis in cerebral endothelial cells (Villaseñor et al., 2019). At their abluminal side, ECs are surrounded by basal lamina embedding pericytes, and interact with glial cells (astrocytic end-feet and microglial cells) and neurons. The whole is called the neurovascular unit (NVU) (Erdő et al., 2017). The presence of glial cells in the vicinity of the BBB promotes NVU susceptibility to neuroinflammatory responses. Neuroinflammation, in turn, can contribute to BBB dysfunction and neurodegenerative process (Vodo et al., 2013).

Androgens were also shown to promote cerebral angiogenesis and vasculature formation, and modulate the cerebrovascular function (see for review, Ahmadpour and Grange-Messent, 2020). In particular, our previous data indicate that gonadal testosterone supports the integrity and function of the BBB and prevents gliosis reaction and the up-regulation of inflammatory proteins in adult male mice (Atallah et al., 2017) and rats (Barreto et al., 2007).

In this context, our work aims to document for the first time the impact of oral exposure during adulthood to low doses of DEHP alone or in a phthalate mixture on the integrity of the capillary BBB and surrounding parenchyma in male mice. Analyses were processed using four experimental groups of adult C57BL/6J male mice exposed orally through contaminated diet in order to mimic the major route of exposure as previously described (Adam et al., 2021). The first three groups included males exposed for 6 weeks to the vehicle (control), DEHP at the TDI dose of 50 µg/kg/d, or DEHP at 5 µg/kg/d. The DEHP dose of 5 µg/kg/d is within the environmental exposure range; this dose induced behavioural alterations in male mice following adult or pubertal exposure (Capela and Mhaouty-Kodja, 2021; Dombret et al., 2017). In order to mimic environmental co-exposure to phthalates (Anses, 2015; Martine et al., 2013), the fourth group of males was exposed for 6 weeks to a phthalate mixture containing DEHP at 5 µg/kg/d, DBP at 0.5 µg/kg/d, BBP at 0.5 µg/kg/d, DiBP at 0.5 µg/kg/d and DEP at 0.25 µg/kg/d. Analyses focused on two androgen-sensitive brain areas as mentioned above the hypothalamic mPOA and the hippocampus. In these brain areas, we investigated the effects of exposure on BBB permeability using exogenous tracer and endogenous immunoglobulins G (IgG). Protein levels and distribution of TJ components as well as glial activation and neuroinflammation were also assessed in the four exposed groups.

# 2. Material and Methods

## 2.1. Ethical statement

The experiments have been reported in compliance with the Animal Research: Reporting in Vivo Experiments (ARRIVE) guidelines. All studies were performed in compliance with the National Institute of Health guidelines for the care and use of Laboratory Animals (NIH Guide) and French and European legal requirements (Decree 2010/63/UE). Experiments were performed accordingly, to minimize animal number and discomfort and were approved by the “Charles Darwin” Ethical committee (project number 01490-01).

## 2.2. Animals

Males of C57BL/6j strain (Janvier Labs, Le Genest-Saint-Isle, France) bred in our laboratory were housed in a conventional facility after weaning under controlled photoperiod (12:12h light dark cycle-lights on at 1 p.m.), maintained at 22°C and relative humidity (60% ± 10%), and had free access to water and a standard diet (A03–10; Safe-diets, Augy, France). The mice were housed in nest-enriched polysulfone cages, with polysulfone bottles. Offspring were mixed at the weaning to avoid potential litter effects with no more than one male per litter per cage, and were allowed to grow to 8 weeks of age. For these experiments, 9 cohorts each comprising 9 to 32 animals distributed equally between the 4 treatment groups, were used. Ultimately, 32 animals from two cohorts were used for BBB permeability assays, 96 animals from five cohorts were used for the capillary-enriched fraction procedure and Western blot analysis, and then 68 animals from three cohorts were used for the immunocytochemistry study.

## 2.3. Phthalate exposure

Exposure to phthalates (Sigma Aldrich, Saint-Quentin Fallavier, France) was performed for 6 weeks as recently described (Adam et al., 2021). The phthalates were first dissolved in absolute ethanol (1% of prepared food) and then in water (40% of prepared food) before incorporated into food as previously described (Adam et al., 2021). Control animals were fed with chow containing the vehicle i.e. ethanol and water (1% and 40% of prepared food, respectively). Eight-week-old males were fed ad libitum with chow consisted of their normal food containing the vehicle (control group), DEHP (CAS 117-81-7) at 50 or 5 µg/kg/d (DEHP-50 and DEHP-5 groups, respectively), or a phthalate mixture (Mix group) containing DEHP at 5 µg/kg/d, DBP (CAS 84-74-2) at 0.5 µg/kg/d, BBP (CAS 85-68-7) at 0.5 µg/kg/d, DiBP (CAS 84-69-5) at 0.5 µg/kg/d and DEP (CAS 84-66-2) at 0.25 µg/kg/d, reconstituted into pellets as precisely described previously (Adam et al., 2021). The composition of the phthalate mixture was based on French and European studies showing an external co-exposure to these molecules and the presence of their metabolites in urinary samples ( Anses, 2015; Dewalque

et al., 2014; Martine et al., 2013). The ratio of DEHP to the other phthalates was determined on the basis of the estimated daily intake in France and Europe (Dewalque et al., 2014; Martine et al., 2013).

Mice were weighed weekly for the duration of the exposure and phthalate doses were adjusted to their body weights and calculated for a daily food intake of 5 g per animal (Dombret et al., 2017), on the basis of previous studies showing this average daily intake for adult mice of 2 to 19 months old (Cheema et al., Br J Nutrition 2019). Body weight was comparable between the four treatment groups on the first and last days of exposure (supplementary Figure S1).

The analyses were performed on 5 cohorts each comprising animals distributed equally between the 4 treatment groups. Briefly, two cohorts were used for BBB permeability assays, two cohorts were used for immunohistochemistry study and then, one was used for the capillary-enriched fraction procedure and Western blot analysis.

## 2.4. BBB permeability assay

The BBB permeability assay was performed using an exogenous tracer binding to serum albumin, the Evans blue dye (Sigma Aldrich, Saint-Quentin Fallavier, France), and endogenous IgG. The BBB restricts the passage of serum proteins such as albumin and endogenous IgG from the blood flow into the interstitial tissue (Saunders et al., 2015).

### *2.4.1. Evans Blue dye injection*

Three awake mice per treatment group were i.p. injected with a 2% Evans Blue solution (4 ml/kg) diluted in normal saline. Three hours later, the mice were deeply anaesthetized with a lethal dose of pentobarbital (120 mg/kg, i.p.), then transcardially perfused with 0.9% saline solution followed by 4% paraformaldehyde (PFA) solution diluted in 0.1M phosphate buffer (PB) pH 7.4. Their brains were carefully removed and post-fixed with the same fixation solution overnight at 4°C. Afterwards, the brains were cryoprotected with a 20% sucrose solution for 24 hrs at 4°C before freezing in isopentane (-30°C) and 8 coronal sections (20

μm thick) included mPOA or hippocampus were cut using a cryostat and mounted on slides. In order to visualize blood vessel walls, all sections were co-stained with anti-laminin rabbit primary antibody (1/100; Table 1) followed by secondary Alexa488-conjugated anti-rabbit IgG (1:1000, Invitrogen, Villebon sur Yvette, France). To avoid the Evans Blue dye spreading and to promote optimal visualization of labelled fine structures, sections were quickly immersed in xylene and mounted with a hydrophobic mounting medium using the method initially developed by Werner et al., (Werner et al., 1997) and modified by (Atallah et al., 2017). The Evans blue dye providing a red fluorescence (Steinwall and Klatzo, 1966), fluorescent signals were observed under a confocal microscope (described below).

#### *2.4.2. Endogenous Immunoglobulin G detection*

Mice (n = 5 per treatment group) were deeply anaesthetized with a lethal dose of pentobarbital (150 mg/kg, i.p.), then were transcardially perfused with 0.9% saline solution followed by 4% PFA solution diluted in 0.1M PB pH7.4. Their brains were carefully removed and post-fixed with the same fixation solution overnight at 4° C. Afterwards, the brains were cryoprotected with a 20% sucrose solution for 24 hrs at 4°C before freezing in isopentane (-30°C) and 8 coronal sections (20 μm thick) included mPOA or hippocampus were cut using a cryostat and mounted on slides. The presence of extravasated endogenous mouse IgG from blood to parenchyma was evaluated using Alexa488-conjugated anti-mouse IgG antibody (1:1000, Invitrogen, Villebon sur Yvette, France) combined with immuno-labelling of laminin as described above to detect microvessels. Then fluorescent staining was observed under a confocal microscope (described below).

### 2.5. Fluorescent immunohistochemistry

The animals (n=5 per treatment group and per immuno-labelling) were deeply anaesthetized with a lethal dose of pentobarbital (120 mg/kg, i.p.) for the following procedures.

#### *2.5.1. Tissue preparation*

The experiments were processed as previously described (Atallah et al., 2017). Briefly, for TJ proteins (claudin-5, occludin and ZO-1) and the main component of caveolae plasma membranes, Cav-1 protein, the brains were freshly removed and immediately frozen in isopentane (−30°C). Six to eight serial frozen sections (20-µm thickness) included mPOA and hippocampus were cut and collected on slides, and were then fixed by immersion for 2 min at −20 ℃ in methanol/acetone (vol/vol) with this followed by the labelling procedure. For the other proteins (Iba-1, GFAP, S100ß, NDRG-2, Cox-2 and iNOS), male mice were deeply anesthetized using i.p. injection of pentobarbital (120 mg/kg) diluted in with 0.9% saline solution and then transcardially perfused with 0.9% saline solution followed by 4% paraformaldehyde solution diluted in 0.1 M PB pH7.4. After post-fixation and cryoprotection steps as described above, the brains were frozen in isopentane (-30°C) and 6 to 8 serial frozen sections (20 µm thickness) included mPOA or hippocampus were cut using a cryostat and collected on slides.

#### *2.5.2. Immuno-labelling procedure*

Non-specific sites were blocked by incubating slide-mounted sections in PBS 1X, 1% bovine serum albumin (BSA) and 0.2% Triton X-100 for 1 h at room temperature. Then sections were incubated with one or more primary antibodies (Table 1) overnight at 4° C diluted in the same phosphate buffer saline (PBS)/bovine serum albumin (BSA)/Triton X-100 solution. Immune complexes were revealed using secondary Alexa-conjugated anti-mouse, anti-goat or anti-rabbit IgG (1:1000; Invitrogen, Villebon sur Yvette, France). Fluorescence was observed with a confocal microscope.

### 2.6. Confocal microscopy

Simple and multiple fluorescent labelling was visualized with a SP5 upright Leica confocal laser scanning microscope (Leica Microsystems) equipped with the Acousto-Optical Beam Splitter (AOBS) and using 63x oil immersion objective. Alexa 488 was excited at 488nm and observed from 495 to 580 nm; Alexa 555 was excited at 555 nm and observed from 599 to

680 nm. The gain and offset for each photomultiplier were adjusted to optimize detection events. Images (1024x1024 pixels, 16 bits) were acquired sequentially between stacks to eliminate cross-over fluorescence. The frequency was set up at 400 Hz and the pinhole was set at 1 Airy. Each optical section (1 µm) was frame-averaged four times to enhance the signal/noise ratio. Overlays, projection of the z-stack files and quantification were performed using the Fiji software (NIH, USA). The presented pictures were the projection of 10–20 successive optical sections into one image, unless otherwise stated in the figure legend. Quantification of the fluorescent density was performed on three sections sampled at the level of the mPOA (plate 30 of the Mouse Brain Atlas of Paxinos and Franklin 2001) and on three sections sampled at the level of the hippocampus (plate 48). The surfaces on which the fluorescence density quantifications were performed are given in the figure legends.

## 2.7. Western blot protein analysis using cerebral capillary-enriched factions

### *2.7.1. Cerebral capillary-enriched fraction procedure*

Brains from 12 mice per treatment group were freshly removed and placed quickly on ice. For each hypothalamic capillary-enriched fraction, two hypothalami were pooled (n = 6 per treatment group), whereas one hippocampus was used for each hippocampal capillary-enriched fraction (n = 6 per treatment group). Hypothalamic and hippocampal microvessels were harvested according to a previously described method (Atallah et al., 2017; Sandoval and Witt, 2011), in order to obtain microvessel-enriched fractions for each cerebral area. Briefly, samples were homogenized in a pH 7.4 buffer containing 1% BSA, 2.7 mM KCl, 137 mM NaCl, 1.5 mM $KH_2PO_4$, 8 mM $Na_2HPO_4$, 1 mM $CaCl_2$, 0.5 mM $MgCl_2$, $6H_2O$, mM D-glucose, 1 mM sodium pyruvate, 1 M 4-(2-Hydroxyethyl) piperazine-1-ethanesulfonic acid (HEPES). Homogenates were centrifuged in an equal volume of 30% Ficoll for 15 min at 4800g at 4°C, supernatants were aspirated and pellets suspended in isolation buffer without BSA and passed through a 70-µm nylon filter. Filtrates were centrifuged for 10 min at 4 °C at 3000g.

### *2.7.2. Protein extraction*

Protein extraction from pellets of microvascular capillary fractions was performed with a RIPA buffer containing 50mM Tris—base (pH 7.2), 10 mM EDTA, 10 mM EGTA, 150 mM NaCl, 0.1% sodium dodecyl sulfate, 0.5% deoxycholate acid, 1% Triton X-100, and 1% protease inhibitor cocktail (Sigma Aldrich) and sonicated 10 times for 30 s. Homogenate samples were centrifuged at 13000 rpm for 13 min at 4 °C and supernatants containing proteins were collected. The total protein concentration of each sample was determined using the Bradford Assay Kit (Thermo Scientific, Courtaboeuf-Villebon sur Yvette, France) according to the manufacturer's protocol. Protein extracts were stored at -20°C until further processing.

### *2.7.3. Electrophoresis and immunoblotting*

Protein samples were denatured in Laemmli Buffer and heated at 95°C for 5 min. Electrophoretic migration of 10–20 µg of proteins was carried out on NuPAGE 4–12% Bis–Tris Gel (Invitrogen, Villebon sur Yvette, France) or Mini-PROTEAN® TGX™ 7.5% polyacrylamide gels (BIO-RAD, Marnes La Coquette, France). The resolved proteins were then electrotransferred onto pre-treated polyvinylidene difluoride (PVDF) membranes (Millipore, Molsheim, France).

Membranes with transferred proteins were blocked for 1 h, at RT with a solution of 5% non-fat milk diluted in PBS 1X with 0.2 % Tween, and then incubated with primary antibodies (Table 1) diluted in the same blocking solution overnight at 4 °C. Primary antibody binding to blots was detected by incubation with respectively either secondary HRP–conjugated (1:5000; Jackson, Cambridgeshire, United Kingdom) or biotin–conjugated (1:2000; Vector, Burlingame, United States,) anti-rabbit, anti-mouse or anti goat for 2 h, at RT, and then immune complexes were revealed by the SuperSignal™ West Pico or Femto Chemiluminescent Substrate kit (Thermo Scientific, Courtaboeuf-Villebon sur Yvette, France).

The signals were quantified by using FiJi software (NIH, USA) and normalized to the value obtained for the corresponding housekeeper glyceraldehyde- 3-phosphate dehydrogenase (GAPDH) protein band.

### 2.8. Statistical analysis

The four sample sizes corresponding to the vehicle-treated, DEHP-5 or DEHP-50 and phthalate mixture were equal. Normal distribution of the four groups was checked using the Shapiro-Wilk normality test then one-way ANOVA was used to analyze the main effects of exposure and Tukey tests were used for posthoc analyses to determine group differences. Differences were considered statistically significant if $p \leq 0.05$. In the text, means ± S.E.M are expressed as a percentage of the vehicle group. Two-way ANOVA was used to analyze the effects of treatment on the body weight of exposed mice. Data are expressed as body weight means (g) ± S.E.M and differences were considered statistically significant if $p \leq 0.05$.

## 3. Results

### 3.1. BBB permeability

BBB permeability in the hypothalamic mPOA and hippocampal CA1, CA3 and DG sub-regions was assessed in mice exposed to the vehicle or DEHP alone or in a phthalate mixture by using exogenous Evans Blue dye (Figure 1; A-H), which binds to albumin protein, and endogenous circulating IgG molecules (Figure 1; I-P). Detection of these tracers in the parenchyma, called extravasation, indicates a BBB leakage. Therefore, to visualize blood capillary walls, laminin, the main basal lamina protein, was immunodetected.

In the hypothalamic mPOA, fluorescent signal analyses showed treatment had had a significant effect ($p \leq 0.01$) on the extravasation of the Evans Blue dye outside perfused brain capillaries, with an increased extravasation in DEHP-5-, DEHP-50- and Mix-treated mice (+110% $p \leq 0.01$, +130% $p \leq 0.01$ and +135% $p \leq 0.001$, respectively, above vehicle-treated mice) determined by posthoc analyses (Figure 1A and B). In the hippocampus, the treatment

was found to have had an effect on the extravasation of the Evans Blue dye in the CA1 and CA3 regions ($p \leq 0.0001$, $p \leq 0.01$, respectively). A significant increase above vehicle-treated mice was evidenced by posthoc analyses for DEHP-5- and DEHP-50-treated mice in the CA1 parenchyma (+95% $p \leq 0.01$ and +170% $p \leq 0.001$ respectively, $p \leq 0.05$), but only for DEHP-50-treated mice in the CA3 parenchyma (+70%, $p \leq 0.05$) (Figure 1 C-F). In contrast, there was no treatment effect in the DG capillaries, which greatly restricted Evans blue dye extravasation to the brain parenchyma (Figure 1G and H).

Immunolabelling of endogenous circulating IgG showed that endogenous IgG were observed and were restricted to capillary wall or lumen in vehicle-treated mice (Figure 1K and M). In contrast, the effect of treatment on IgG immunoreactivity in the mPOA ($p \leq 0.01$), with higher levels in DEHP-5, DEHP-50- and mixture-treated mice (+160%, $p \leq 0.01$; +35% and +15%, $p \leq 0.05$; respectively) in the parenchyma of phthalate-treated mice compared to the vehicle group (Figure 1I and J) was shown by posthoc analyses. Similarly, a treatment effect ($p \leq 0.0001$) was found in the CA1 area with significantly higher levels of endogenous IgG in the DEHP-5 (+140 %, $p < 0.05$), DEHP-50 (+270 %, $p < 0.01$) and Mix-groups (+900 %, $p < 0.0001$) versus the vehicle group (Figure 1K and L) was shown by posthoc analyses. There was also a treatment effect in the CA3 area ($p \leq 0.0001$) as illustrated in Figure 1M and N; posthoc analyses showed increased levels for mice exposed to DEHP alone or in a mixture (+ 86%, +89% and +100%, $p \leq 0.0001$, for DEHP-5, DEHP-50 and mixture-group vs. vehicle, respectively). In accordance with the result obtained for Evans blue dye, no extravasation of circulating IgG from blood compartment to hippocampal DG parenchyma was detected (Figure 1O and P).

### 3.2. Protein levels and distribution of TJ components

BBB leakage induced by DEHP alone or in a mixture could be due to an alteration of capillary inter-endothelial TJs leading to paracellular transport of components. TJs comprise a complex of transmembrane proteins claudin-5 and occludin, which are associated with peripheral scaffolding proteins. Therefore, we investigated the distribution and amounts of

these proteins using immunofluorescence and Western blot analysis on microvessel-enriched fractions. No significant effect of treatment was found on the protein amounts of claudin-5 and occludin in the capillaries of hypothalamus (Figure 2A and B) and hippocampus (Figure 2D and E). In addition, confocal microscopy analysis of the capillaries of hypothalamic mPOA and hippocampal CA1, CA3 and DG sub-regions, showed no significant treatment effect on the distribution of immuno-labelling of claudin-5 (supplementary figure S2) and occludin (supplementary Figure S3).

Those endothelial transmembrane components of TJs interact with the actin cytoskeleton via cytoplasmic TJs accessory proteins with the ZO-1 protein having predominance. Data from Western blot performed on microvessel-enriched fractions obtained from the hypothalamus (Figure 2C), highlighted a treatment effect on ZO-1 protein amount ($p \leq 0.0001$), with less ZO-1 for both DEHP-5- and DEHP-50-treated mice (-75%, $p \leq 0.0001$) and also Mix-treated mice (-65%, $p \leq 0.0001$) versus the vehicle group following posthoc analyses. A treatment effect was also found on the amount of ZO-1 in hippocampal capillaries (Figure 2F). Posthoc analyses showed that the amount of ZO-1 was significantly increased for DEHP-50- treated mice (+50%, $p \leq 0.05$), whereas no significant difference was detected for DEHP-5- and mixture-treated groups compared to vehicle (Figure 2F). As for claudin-5 and occludin, confocal microscopy analysis of the capillaries of hypothalamic mPOA and hippocampal CA1, CA3 and DG sub-regions, showed no treatment effect on the immuno-labelling of ZO-1 protein (supplementary Figure S4).

### 3.3. Cav-1 protein level in capillaries walls

Caveolae are non-clathrin-coated vesicles with plasma membranes enriched in caveolin (Cav) proteins, involved in the receptor-independent transcellular transport of molecules from blood to parenchyma. We analyzed the level of caveolin-1 isoform protein (Cav-1), the main component of the caveolae plasma membranes. Fluorescence analysis revealed an effect of treatment ($p \leq 0.01$) on Cav-1 immunoreactivity in capillary walls and posthoc analyses showed a significant high decrease for DEHP-50- and Mix-treated mice in the mPOA (DEHP-

50 group: -50 %; $p < 0.05$ and mixture-group: -75%; $p < 0.01$ vs. vehicle; Figure 3A and B) and in the CA-1 (DEHP-50 group: -60 %; $p < 0.05$ and mixture-group: -70%; $p < 0.01$ vs. vehicle; Figure 3D and E) and CA-3 areas (-70 %; $p < 0.01$ vs. vehicle in DEHP-50 and mixture-group; Figure 3F and G). Again, no significant treatment effect was found in hippocampal DG (Figure 3H and I). These results were confirmed by Western blot analysis performed on microvessel-enriched fractions showing a treatment effect ($p \leq 0.001$), with a decrease by -63% and -56% ($p < 0.01$ in DEHP-50 and mixture-group, respectively) in hypothalamic vessels (Figure 3C) and -60% ($p < 0.01$) and -50% ($p < 0.05$) in hippocampal vessels of DEHP-50 and mixture-group respectively in comparison to the vehicle group (Figure 3J) determined by posthoc analyses.

### 3.4. Glial activation and neuroinflammation

The neuroinflammation process occurs following several brain insults and is often associated with a dysfunction of the neurovascular unit. Neuroinflammatory responses are underlined on the one hand by a glial activation involving an increase of glial specific protein levels, NDRG2, S100ß and GFAP for astrocyte, and Iba-1 for microglia, and on the other hand by an increase of inflammatory molecules such as iNOS and COX-2. The distribution of these proteins was assessed using immunofluorescence, and protein levels in glial cells closely associated with capillaries were assessed using Western blot analysis performed on microvessel-enriched fractions from the whole hypothalamus and hippocampus.

In the mPOA, analyses of immunofluorescence results showed an effect of treatment on NDRG2 and S100ß labellings ($p \leq 0.0001$; $p \leq 0.05$, respectively). A significant increase of NDRG2 labelling in astrocytes for mixture-treated mice (+125%, $p < 0.0001$ vs. vehicle, Figure 4A and B) and a significant increase of S100ß labelling in astrocytes for DEHP-50- and mixture-treated mice (+92% and +82% vs. vehicle, respectively, $p < 0.05$, Figure 4A and C) were determined by posthoc analyses. All NDRG2-positive astrocytes are immunoreactive for S100ß but few S100ß-positive astrocytes express NDRG2. This astrocytic activation was confirmed by a significant enhancement of GFAP immunofluorescence density in the

parenchyma and in the vicinity of capillaries for DEHP-50-treated mice (+ 100%; $p < 0.05$ vs. vehicle, Figure 4D and E). By contrast, Western blot analysis performed on microvessel-enriched fractions showed an effect of treatment ($p \leq 0.0001$), with a significant decrease of GFAP amount in the astrocytic end-feet which remained in contact with the isolated vessels for DEHP-5-, DEHP-50- and mixture-treated mice compared to vehicle (-40%, $p < 0.01$, -55%, $p < 0.0001$ and -37%, $p < 0.01$, respectively vs. vehicle, Figure 4G), determined by posthoc analyses.

Immunofluorescent analysis showed an effect of treatment ($p \leq 0.01$), with a stronger signal for iNOS colocalized with GFAP surrounding capillaries not only for DEHP-5-, DEHP-50-treated mice (+280 %; $p < 0.01$ vs. vehicle) but also for mixture-treated mice compared to vehicle (+360 %; $p < 0.001$ vs. vehicle) (Figure 4D and F). Conversely, no significant effect was highlighted for iNOS protein level using Western blot analysis performed on hypothalamic microvessel-enriched fractions (Figure 4H). Immunohistochemical labelling for the specific marker of microglial cells, Iba-1, was also changed by the treatment ($p \leq 0.01$) and posthoc analyses showed a significant increase in the mPOA parenchyma for DEHP-50-treated mice (+125%; $p < 0.01$ vs. vehicle, Figure 6A and B), whereas hypothalamus capillary-enriched fraction showed no difference in the amount of Iba-1 protein among the experimental groups (Figure 6C). COX-2 protein was immuno-detected in Iba-1-immunopositive microglial cells in the mPOA (Figure 6A) especially for DEHP-50-treated group compared to vehicle (+130 %; $p < 0.01$, Figure 6D). However, no significant difference in the COX-2 protein amount was measured in the capillaries of hypothalamus of phthalate-treated mice compared to those of vehicle-treated mice (Figure 6E).

In the hippocampus, analysis of the environment of the capillaries of CA1, CA3 and DG sub-regions showed no significant treatment effect for immuno-labelling intensity of NDRG2 and S100ß for all phthalate-treated groups compared to the vehicle (Figure 5A-F). Observations using confocal microscopy confirmed these results (supplementary figure S5). Quantification of GFAP immunoreactivity displayed no significant treatment effect between control and

phthalate-treated mice not only in the CA1 (Figure 5G and H) but also in the CA3 (Figure 5J and K) and in the DG region (Figure 5M and N). Western blot analysis performed on hippocampal microvessel-enriched fractions did not show any modification of GFAP protein content in the hippocampus, regardless of the experimental group (Figure 5P). Immunofluorescent analysis showed that iNOS labelling was not co-localized with GFAP labelling in the CA1 region (Figure 5G), but was significantly impacted by the treatment ($p \leq 0.01$) and enhanced for DEHP-5-, DEHP-50 and mixture-treated mice compared to the vehicle (+180 %; $p < 0.01$, +125 %; $p < 0.05$, and +115 %; $p < 0.05$, respectively vs. vehicle, Figure 5I) determined by posthoc analyses. In the hippocampal CA3 region, the level of iNOS immunoreactivity, not detected in astrocyte (Figure 5J), was equivalent between animals treated with the vehicle and DEHP alone or in a mixture (Figure 5L). In the hippocampal DG, iNOS immunoreactivity was affected by the treatment ($p \leq 0.001$) and significantly increased only for DEHP-5-treated mice (+270%; $p < 0.001$, vs. vehicle, Figure 5O). Finally, no effect on iNOS protein amount was measured (Figure 5Q) in the hippocampal microvessels.

Iba-1 immunoreactivity was affected by treatment ($p \leq 0.05$) and increased in the CA1 (+115%, + 125% and + 118%; $p < 0.05$ vs. vehicle in DEHP-5, DEHP-50 and mixture-group respectively; Figure 6F and G), and in CA3 areas (DEHP-5 group: + 200%; $p < 0.0001$; DEHP-50 group: + 90 %; $p < 0.05$; mixture-group: + 80%; $p < 0.05$ vs. vehicle; Figure 6I and J). No treatment effect was measured in the DG (Figure L and M). In the hippocampal capillaries-enriched fractions, no significant treatment effect was observed on the protein amounts of Iba-1 (Figure 6O). Confocal microscopy and Western blot analysis showed no significant effect on COX-2 immunolabelling (Figure 6H, K and N) and the amount of protein in microvessel-enriched fractions of the hippocampus (Figure 6P).

## 4. Discussion

This study aimed to characterize the impact of a subchronic oral exposure to environmental doses of DEHP alone or in a phthalate mixture on the neurovascular unit in the hypothalamus and hippocampus of adult male mice. To our knowledge of the available literature, this study is the first to assess the effects of adult exposure to low doses of phthalates on the blood-brain barrier.

The data obtained show that exposure to DEHP alone or in a phthalate mixture significantly increased the BBB permeability in the hypothalamic mPOA and the hippocampal CA1 and CA3 regions as evidenced by the use of two different techniques assessing extravasation of exogenous Evans blue tracer and circulating endogenous IgG. It is generally accepted that increased permeability of the BBB reflects the failure of its functional integrity (Erdő et al., 2017), which can be manifested by an alteration at the molecular and / or morphological level of the constituents of these TJs (Obermeier et al., 2013). Our results show that exposure to DEHP alone or in a phthalate mixture did not affect the expression of the major TJs transmembrane proteins, claudin-5 and occludin, indicating that the increased BBB permissiveness was not due to changes in these protein amounts in the two brain structures we assessed. Our results show that the increased BBB permeability induced by exposure to DEHP alone at 5 or 50 µg/kg/d or DEHP 5 µg/kg/d in a phthalate mixture was associated with a dramatically decreased amount of the accessory junctional protein ZO-1 in hypothalamic microvessel-enriched fractions. An opposite effect was observed in hippocampal microvessel-enriched fractions in the group exposed to DEHP at 50 µg/kg/d. The underlying cause of these changes could, at least in part, be the observed BBB integrity failure induced by exposure to DEHP alone or in a mixture, since interaction between claudin, occludin and ZO-1 is pivotal for facilitating tight junction assembly, and regulating the effectiveness of TJs complex function (Abbott et al., 2010). However, it is important to note that no difference was detected in ZO-1 immunoreactivity when assessed by immunohistochemistry in the mPOA, or CA1 and CA3 regions. A possible explanation could be that in the brain sections submitted to immunohistochemical analyses, the quantifications were carried out from 2-dimensional

images and therefore the absence of the third dimension may impede the complete evaluation of the components of TJ proteins.

In addition to this possible impairment in the organization of endothelial TJs, our results also highlight potential modifications in caveolae-mediated transcellular transport. Indeed, adult exposure to DEHP at 50 µg/kg /d or to DEHP 5 µg/kg /d in the phthalate mixture led to a significant decrease in Cav-1 immunoreactivity in the mPOA and CA1 and CA3 regions, and in the amount of protein of the microvessel-enriched fractions of the hypothalamus and hippocampus.

In the DG, none of the modifications induced by phthalate exposure on BBB permeability and amounts of proteins involved in endothelial TJs and Cav-1 were observed, indicating that BBB integrity was preserved in this hippocampal vascular network. These results suggest that, within the same brain structure, the BBB may exhibit differential sensitivity to exposure to DEHP alone or in a mixture. This difference in sensitivity within the hippocampus suggests that maintaining BBB would involve different signalling pathways, with the DG containing neural circuits different from those of the CA1 and CA3 subregions and being the site of adult neurogenesis.

The modifications induced by exposure to DEHP alone or in a phthalate mixture in the BBB integrity were associated with astrocyte and microglial activation in the hypothalamic mPOA. Astrocyte activation was characterized by the increased immunoreactivity for both GFAP, NDRG2 and S100ß in the parenchyma of the mPOA. Firstly, this is in accordance with our recent study reporting that chronic adult exposure to DEHP at 50 µg/kg/d induced an up-regulation of GFAP in the parenchyma of the mPOA in male mice (Dombret et al., 2017). Secondly, the data also indicate that adult exposure of male mice to DEHP alone or in a phthalate mixture was capable of affecting different steps of cellular activation and states. NDRG2 is induced in the early phase of astrocyte activation preceding GFAP expression (Lin et al., 2015), while S100ß is defined as a state in which astrocytes lose their neural stem cell potential and acquire a more mature developmental stage (Raponi et al., 2007). Western blot

analysis performed with hypothalamic microvessel-enriched fractions showed a decreased GFAP amount in astrocyte end-feet associated with microvessels. This difference in the data protein obtained between the two techniques suggests a reorganization of the intermediate filament cytoskeleton of astrocytes involved in the BBB. Reactive astrocytes are known to express the pro-inflammatory molecule iNOS in response to various stimuli to produce an excessive amount of nitric oxide (NO), a gaseous signalling molecule involved in most cases with a neurodegenerative and neuroinflammatory status (Saha and Pahan, 2006). A Western blot performed on microvessel-enriched fractions from the whole hypothalamus showed no changes in the iNOS protein levels, but higher iNOS labelling was colocalized with GFAP labelling astrocyte end-feet associated with capillaries in the mPOA. This suggests that the inflammatory reaction mediated by astrocytes was initiated at, or limited to, the level of the BBB. The astroglial activation in the parenchyma of the mPOA induced by the exposure to DEHP at 50 µg/kg/d was accompanied by an activation of microglial cells, which also exhibited a higher immunoreactivity of the inflammatory molecule COX-2. The association between COX-2 expression and microglial activation could lead to NVU impairment through neuronal damage as has been previously reported (Vijitruth et al., 2006). Further studies will compare the impact of phthalate exposure on neuronal integrity.

In the hippocampus, no changes in astrocyte activation markers were induced by adult exposure to DEHP alone or in a phthalate mixture, suggesting an absence of astrocyte activation in this region despite the increased BBB permeability. In contrast, microglial activation was observed in the CA1 and CA3 sub-regions following exposure to DEHP alone or in a phthalate mixture, whereas no changes in COX-2 immunoreactivity were demonstrated. A recent investigation has shown that prenatal exposure to DEHP at 200 µg/kg/d increased the level of COX-2 in pyramidal neurons of the CA-2/3 region in adult male mice (Barakat et al., 2018). This suggests that differences in induced COX-2 expression by phthalates may depend on the period of exposure. Alternatively, a longer exposure period in adult males may be a more efficient way of inducing astrocyte activation and COX2

518 expression. Nevertheless, exposure to DEHP alone or in a mixture-induced iNOS activation
519 was noted in the CA1 and DG sub-regions but not in the CA3 area, while BBB leakage was
520 detected in both the CA1 and CA3 areas. The iNOS labelling was thus not colocalized with
521 the astrocytic marker GFAP, suggesting that astrocytes of the BBB may not be the only cells
522 capable of producing NO under these conditions. Indeed, different brain cell types including
523 neurons, macrophages and microglia, can respond to different stimuli with iNOS production
524 and take part in brain inflammation (Heneka and Feinstein, 2001; Sierra et al., 2014). It is
525 thus possible that an increased amount of iNOS protein in the hippocampus may arise from
526 an additional direct impact of DEHP alone or in a mixture on the parenchyma. Phthalates are
527 able to cross the BBB thus eliciting direct effects through neuronal damage,
528 neuroinflammation, oxidative stress and alteration of monoaminergic, cholinergic and amino-
529 acids transmission as has been reported for adult or developmental exposure to DEHP or
530 DBP at high doses ranging from 30 to 750 mg/kg/d (Kassab et al., 2019; You et al., 2018).
531 Thus, the question remains as to whether the BBB dysfunction is a cause or a consequence
532 of a neuroinflammatory state.

533 Altogether, these data show that the BBB dysfunction and generally associated astroglial
534 activation and neuroinflammation were differently induced by adult exposure to DEHP alone
535 or in a phthalate mixture (Table 2). Differences were seen between the hypothalamic mPOA
536 and hippocampus, in particular for the astrocyte activation. Differences in sensitivity to
537 exposure were also suggested by the obtained data for each brain area. In the mPOA, while
538 BBB permeability and iNOS induction were affected since 5 µg/kg/d of DEHP alone or in a
539 mixture, the other parameters were rather altered at 50 µg/kg/d of DEHP and /or the mixture,
540 suggesting that the other phthalates add to the effects of DEHP-5. In the hippocampus, the
541 DG appeared less sensitive showing only an induced iNOS in response to DEHP treatment
542 while the CA1 and CA3 areas were more reactive, with effects induced since 5 µg/kg/d of
543 DEHP alone for BBB permeability, microglial activation and neuroinflammation.

The down-regulation of the androgen receptor (AR) induced by exposure to DEHP in the hypothalamic mPOA has been previously shown (Dombret et al., 2017). Thus, the alterations triggered by adult exposure to DEHP alone or in a phthalate mixture in the neurovascular unit of the mPOA may be also linked, at least in part, to the down-regulation of the AR. Furthermore, in another study, we have shown that testosterone depletion in adult male mice, leading to a down-regulation of the neural AR, triggered i) BBB permeability for Evans Blue and endogenous IgG with a disorganization of TJ structure including a reduced protein amount of ZO-1, ii) increased activation of astrocytes and microglia and iii) up-regulation of inflammatory molecules such as iNOs and COX2 (Atallah et al., 2017). Finally, the AR mediated-transcriptional activity is, at least in part, positively modulated by the caveolae transmembrane Cav-1 protein (Bennett et al., 2010; Lu et al., 2001). The tight regulation by androgens of several proteins involved in these processes is detailed in a recent review (Ahmadpour and Grange-Messent, 2020).

The hippocampus is also an androgen-sensitive area, as evidenced by a high AR expression in male mice and altered related functions in a mouse model lacking the neural *A*R (Mhaouty-Kodja, 2018; Picot et al., 2016; Raskin et al., 2009). It is thus possible that the alterations reported here in the neurovascular unit of this structure may also depend, at least in part, on an impact on the AR signalling pathway. This can explain the comparable data obtained on BBB permeability, endothelial TJs and trans-endothelial vesicular transport in the mPOA and CA1 and CA3 regions following exposure to DEHP alone or in a phthalate mixture (Table 2). The CA1 and CA3 regions contain much more AR-immunoreactive neurons than the DG (Raskin et al., 2009), which may explain the reduced sensitivity of this latter area to DEHP exposure.

The differences observed in astrocyte activation and COX-2 expression between the mPOA and the hippocampal CA1 and CA3 regions, and also within the same brain area for the different components of the neurovascular unit could be underlined by different expression patterns of AR but also of estrogen receptors (ERs) in neurons, endothelial cells, astrocytes

571 and microglia, which also express these receptors (Hajszan et al., 2007; Kerr et al., 1995;
572 Picot et al., 2016). Indeed, in the male rodent nervous system, testosterone exerts its effects
573 through direct activation of the AR, but can also be metabolized into estradiol, which then
574 stimulates ERα and ERβ.

575 The effects induced by DEHP exposure i.e. BBB permeability, astroglial activation and
576 neuroinflammation in adult male mice may participate, in particular in the mPOA, to the
577 altered sexual behaviour observed under similar experimental conditions (Dombret et al.,
578 2017). Current studies explore the cognitive impact of male mice exposure to low doses of
579 phthalate but only one recent study addressed the effects of adult DEHP exposure on spatial
580 learning and memory at high doses of 100 and 300 mg/kg/d in male rats (Ran et al., 2019).
581 Besides behavioural alterations, the BBB leakage and inflammatory signs induced by oral
582 exposure to low doses of phthalates reported in the present study may participate in other
583 neural alterations. Although they appear moderate, these modifications could have
584 deleterious long-term consequences in the case of chronic environmental exposure. Indeed,
585 BBB impairment and neuroinflammation are suspected to be involved in neurodegenerative
586 diseases and aging processes (Erdő et al., 2017).

587 Our analyses addressing the impact of DEHP exposure on behavioural responses (Dombret
588 et al., 2017) and BBB integrity (present study) in male mice show that DEHP-induced effects
589 can be observed at low doses equivalent or below the tolerable daily intake dose of 50
590 µg/kg/d, which was established and recently updated by the European Food Safety Authority
591 on the basis of reduced fetal testosterone production. This indicates that the nervous system
592 including the neurovascular unit is highly sensitive to phthalates and should be also
593 considered as a relevant endpoint in risk assessment for these molecules. In this context, it
594 is important to stress that the human cerebrovascular function also seems sensitive to
595 androgen, although these effects are less defined than for estrogens (see for review,
596 (Robison et al., 2019)).

597 ## 5. Conclusion

The present study shows that phthalates, a family of endocrine disruptors, can impact the cerebrovascular function at doses close to the environmental exposure in adult male mice. Subchronic exposure to low doses of DEHP alone or in a phthalate mixture increases BBB permeability of two brain regions leading to a dysfunctionality of this selective interface, which is needed to ensure a tight regulation between the circulatory system, the immune system and the brain parenchyma. In addition, we also show similarities and differences in the vulnerability of the NVU of the two brain regions, one controlling male sexual behaviour, and the second one involved in cognitive function. Based on our previous studies, we suggest that phthalates may operate through a mode of action involving at least a partial disruption of neural *AR* expression in the mPOA, but the ER and/or other signalling pathways may be also involved in the hippocampus.

These data suggest that exposure to endocrine disruptors may be considered as an environmental risk factor for the cerebrovascular function.

## Author contributions

**Delnia Ahmadpour**: Investigation, Formal analysis, Writing-original draft**. Valérie Grange-Messent**: Conceptualization, Supervision, Writing-review & editing. **Sakina Mhaouty-Kodja**: Funding acquisition, Review & editing.

## Declaration of Interest Statement

The authors declare they have no actual or potential competing financial interests or personal relationships that could have appeared to influence the work reported in this paper.

## Acknowledgments

This work was supported by the Agence Nationale de la Recherche (Phtailure, 2018). We thank the rodent facility of the Institut de Biologie Paris-Seine (IBPS, Paris, France) for taking care of the animals and the IBPS Imaging facility (confocal microscopy).

## References

Abbott, N.J., Patabendige, A.A.K., Dolman, D.E.M., Yusof, S.R., Begley, D.J., 2010. Structure and function of the blood-brain barrier. Neurobiol. Dis. 37, 13–25. https://doi.org/10.1016/j.nbd.2009.07.030

Adam, N, Brusamonti, L, Mhaouty-Kodja, S., 2021. Exposure of adult female mice to low doses of di(2 ethylhexyl)phthalate alone or in an environmental phthalate mixture: Evaluation of reproductive behavior and underlying neural mechanisms. Environ Health Perspect, 129 (1). https://doi.org/10.1289/EHP7662

Ahmadpour, D., Grange-Messent, V., 2020. Involvement of testosterone signaling in the integrity of the neurovascular unit in the male: review of evidence, contradictions and hypothesis. Neuroendocrinology. https://doi.org/10.1159/000509218

Anses. 2015. Connaissances relatives à la réglementation, à l'identification, aux propriétés chimiques, à la production et aux usages des composés de la famille des Phtalates (Tome3). https://www.anses.fr/fr/system/files/SUBCHIM2009sa0331Ra-106.pdf

Atallah, A., Mhaouty-Kodja, S., Grange-Messent, V., 2017. Chronic depletion of gonadal testosterone leads to blood–brain barrier dysfunction and inflammation in male mice. J. Cereb. Blood Flow Metab. 37, 3161–3175. https://doi.org/10.1177/0271678X16683961

Barakat, R., Lin, P.-C., Park, C.J., Best-Popescu, C., Bakry, H.H., Abosalem, M.E., Abdelaleem, N.M., Flaws, J.A., Ko, C., 2018. Prenatal Exposure to DEHP Induces Neuronal Degeneration and Neurobehavioral Abnormalities in Adult Male Mice. Toxicol. Sci. Off. J. Soc. Toxicol. 164, 439–452. https://doi.org/10.1093/toxsci/kfy103

Barreto, G., Veiga, S., Azcoitia, I., Garcia-Segura, L.M., Garcia-Ovejero, D., 2007. Testosterone decreases reactive astroglia and reactive microglia after brain injury in male rats: role of its metabolites, oestradiol and dihydrotestosterone: Testosterone down regulates reactive gliosis. Eur. J. Neurosci. 25, 3039–3046. https://doi.org/10.1111/j.1460-9568.2007.05563.x

Bennett, N.C., Gardiner, R.A., Hooper, J.D., Johnson, D.W., Gobe, G.C., 2010. Molecular cell biology of androgen receptor signalling. Int. J. Biochem. Cell Biol. 42, 813–827. https://doi.org/10.1016/j.biocel.2009.11.013

Capela, D., Mhaouty-Kodja, S., 2021. Effects of pubertal exposure to low doses of di-(2-ethylexyl)phthalate on reproductive behaviors in male mice. Chemosphere 263, 128191. https://doi.org/10.1016/j.chemosphere.2020.128191

Cheema, U.B., Most, E., Eder, K., Ringseis, R., 2019. Effect of lifelong carnitine supplementation on plasma and tissue carnitine status, hepatic lipid metabolism and stress signalling pathways and skeletal muscle transcriptome in mice at advanced age. Br. J. Nutrition 121 (12), 1323-1333. https://doi.org/10.1017/S0007114519000709

Directive 2013/39/EU of the European Parliament and of the Council amending Directives 428 2000/60/EC and 2008/105/EC as regards priority substances in the field of water policy. Available 429 at: https://www.ecolex.org/details/legislation/directive-201339eu-of-the-european-parliament-and430 of-the-council-amending-directives-200060ec-and-2008105ec-as-regards-priority-substances-in-the431 field-of-water-policy-lex-faoc127344/.

Dewalque, L., Charlier, C., Pirard, C., 2014. Estimated daily intake and cumulative risk assessment of phthalate diesters in a Belgian general population. Toxicol. Lett. 231, 161–168. https://doi.org/10.1016/j.toxlet.2014.06.028

671 Dombret, C., Capela, D., Poissenot, K., Parmentier, C., Bergsten, E., Pionneau, C.,
672 Chardonnet, S., Hardin-Pouzet, H., Grange-Messent, V., Keller, M., Franceschini, I.,
673 Mhaouty-Kodja, S., 2017. Neural Mechanisms Underlying the Disruption of Male Courtship
674 Behavior by Adult Exposure to Di(2-ethylhexyl) Phthalate in Mice. Environ. Health Perspect.
675 125, 097001. https://doi.org/10.1289/EHP1443

676 EFSA (European Food Safety Authority). 2005. Opinion of the Scientific Panel on food
677 additives, flavourings, processing aids and materials in contact with food (AFC) on a request
678 from the Commission related to bis(2-ethylhexyl)phthalate (DEHP) for use in food contact
679 materials. EFSA Journal 3:243; doi: 10.2903/j.efsa.2005.243

680 EFSA (European Food Safety Authority). 2019. Update of the risk assessment of di-
681 butylphthalate (DBP), butyl-benzyl-phthalate (BBP), bis(2-ethylhexyl)phthalate (DEHP), di-
682 isononylphthalate (DINP) and di-isodecylphthalate (DIDP) for use in food contact materials.
683 EFSA Journal, 17:5838; doi: 10.2903/j.efsa.2019.5838

684 Erdő, F., Denes, L., de Lange, E., 2017. Age-associated physiological and pathological
685 changes at the blood-brain barrier: A review. J. Cereb. Blood Flow Metab. Off. J. Int. Soc.
686 Cereb. Blood Flow Metab. 37, 4–24. https://doi.org/10.1177/0271678X16679420

687 Gao, D.-W., Wen, Z.-D., 2016. Phthalate esters in the environment: A critical review of their
688 occurrence, biodegradation, and removal during wastewater treatment processes. Sci. Total
689 Environ. 541, 986–1001. https://doi.org/10.1016/j.scitotenv.2015.09.148

690 Hajszan, T., Milner, T.A., Leranth, C., 2007. Sex Steroids and the Dentate Gyrus. Prog. Brain
691 Res. 163C, 399–816. https://doi.org/10.1016/S0079-6123(07)63023-4

692 Heneka, M.T., Feinstein, D.L., 2001. Expression and function of inducible nitric oxide
693 synthase in neurons. J. Neuroimmunol. 114, 8–18. https://doi.org/10.1016/s0165-
694 5728(01)00246-6

695 Kabir, E.R., Rahman, M.S., Rahman, I., 2015. A review on endocrine disruptors and their
696 possible impacts on human health. Environ. Toxicol. Pharmacol. 40, 241–258.
697 https://doi.org/10.1016/j.etap.2015.06.009

698 Kassab, R.B., Lokman, M.S., Essawy, E.A., 2019. Neurochemical alterations following the
699 exposure to di-n-butyl phthalate in rats. Metab. Brain Dis. 34, 235–244.
700 https://doi.org/10.1007/s11011-018-0341-0

701 Kerr, J.E., Allore, R.J., Beck, S.G., Handa, R.J., 1995. Distribution and hormonal regulation
702 of androgen receptor (AR) and AR messenger ribonucleic acid in the rat hippocampus.
703 Endocrinology 136, 3213–3221. https://doi.org/10.1210/endo.136.8.7628354

704 Lin, K., Yin, A., Yao, L., Li, Y., 2015. N-myc downstream-regulated gene 2 in the nervous
705 system: from expression pattern to function. Acta Biochim. Biophys. Sin. 47, 761–766.
706 https://doi.org/10.1093/abbs/gmv082

707 Lu, M.L., Schneider, M.C., Zheng, Y., Zhang, X., Richie, J.P., 2001. Caveolin-1 Interacts with
708 Androgen Receptor A POSITIVE MODULATOR OF ANDROGEN RECEPTOR MEDIATED
709 TRANSACTIVATION. J. Biol. Chem. 276, 13442–13451.
710 https://doi.org/10.1074/jbc.M006598200

711 Martine, B., Marie-Jeanne, T., Cendrine, D., Fabrice, A., Marc, C., 2013. Assessment of
712 Adult Human Exposure to Phthalate Esters in the Urban Centre of Paris (France). Bull.
713 Environ. Contam. Toxicol. 90, 91–96. https://doi.org/10.1007/s00128-012-0859-5

714 Mhaouty-Kodja, S., 2018. Role of the androgen receptor in the central nervous system. Mol.
715 Cell. Endocrinol. 465, 103–112. https://doi.org/10.1016/j.mce.2017.08.001

716 Obermeier, B., Daneman, R., Ransohoff, R.M., 2013. Development, maintenance and
717 disruption of the blood-brain barrier. Nat. Med. 19, 1584–1596.
718 https://doi.org/10.1038/nm.3407

719 Picot, M., Billard, J.-M., Dombret, C., Albac, C., Karameh, N., Daumas, S., Hardin-Pouzet,
720 H., Mhaouty-Kodja, S., 2016. Neural Androgen Receptor Deletion Impairs the Temporal
721 Processing of Objects and Hippocampal CA1-Dependent Mechanisms. PLoS ONE 11.
722 https://doi.org/10.1371/journal.pone.0148328

723 Ran, D., Luo, Y., Gan, Z., Liu, J., Yang, J., 2019. Neural mechanisms underlying the deficit of
724 learning and memory by exposure to Di(2-ethylhexyl) phthalate in rats. Ecotoxicol. Environ.
725 Saf. 174, 58–65. https://doi.org/10.1016/j.ecoenv.2019.02.043

726 Raponi, E., Agenes, F., Delphin, C., Assard, N., Baudier, J., Legraverend, C., Deloulme, J.-
727 C., 2007. S100B expression defines a state in which GFAP-expressing cells lose their neural
728 stem cell potential and acquire a more mature developmental stage. Glia 55, 165–177.
729 https://doi.org/10.1002/glia.20445

730 Raskin, K., de Gendt, K., Duittoz, A., Liere, P., Verhoeven, G., Tronche, F., Mhaouty-Kodja,
731 S., 2009. Conditional inactivation of androgen receptor gene in the nervous system: effects
732 on male behavioral and neuroendocrine responses. J. Neurosci. Off. J. Soc. Neurosci. 29,
733 4461–4470. https://doi.org/10.1523/JNEUROSCI.0296-09.2009

734 Robison, L.S., Gannon, O.J., Salinero, A.E., Zuloaga, K.L., 2019. Contributions of sex to
735 cerebrovascular function and pathology. Brain Res. 1710, 43–60.
736 https://doi.org/10.1016/j.brainres.2018.12.030

737 Saha, R.N., Pahan, K., 2006. Signals for the induction of nitric oxide synthase in astrocytes.
738 Neurochem. Int. 49, 154–163. https://doi.org/10.1016/j.neuint.2006.04.007

739 Sandoval, K.E., Witt, K.A., 2011. Age and 17β-estradiol effects on blood-brain barrier tight
740 junction and estrogen receptor proteins in ovariectomized rats. Microvasc. Res. 81, 198–205.
741 https://doi.org/10.1016/j.mvr.2010.12.007

742 Saunders, N.R., Dziegielewska, K.M., Møllgård, K., Habgood, M.D., 2015. Markers for blood-
743 brain barrier integrity: how appropriate is Evans blue in the twenty-first century and what are
744 the alternatives? Front. Neurosci. 9. https://doi.org/10.3389/fnins.2015.00385

745 Sierra, A., Navascués, J., Cuadros, M.A., Calvente, R., Martín-Oliva, D., Ferrer-Martín, R.M.,
746 Martín-Estebané, M., Carrasco, M.-C., Marín-Teva, J.L., 2014. Expression of Inducible Nitric
747 Oxide Synthase (iNOS) in Microglia of the Developing Quail Retina. PLoS ONE 9.
748 https://doi.org/10.1371/journal.pone.0106048

749 Steinwall, O., Klatzo, I., 1966. Selective vulnerability of the blood brain barrier in chemically
750 induced lesions. J. Neuropath. Exp. Neurol. 25,: 542-559. https://doi.org/10.1097/00005072-
751 196610000-00004

752 Vijitruth, R., Liu, M., Choi, D.-Y., Nguyen, X.V., Hunter, R.L., Bing, G., 2006.
753 Cyclooxygenase-2 mediates microglial activation and secondary dopaminergic cell death in
754 the mouse MPTP model of Parkinson's disease. J. Neuroinflammation 3, 6.
755 https://doi.org/10.1186/1742-2094-3-6

756 Villaseñor, R., Lampe, J., Schwaninger, M., Collin, L., 2019. Intracellular transport and
757 regulation of transcytosis across the blood–brain barrier. Cell. Mol. Life Sci. 76, 1081–1092.
758 https://doi.org/10.1007/s00018-018-2982-x

759 Vodo, S., Bechi, N., Petroni, A., Muscoli, C., Aloisi, A.M., 2013. Testosterone-Induced Effects
760 on Lipids and Inflammation [WWW Document]. Mediators Inflamm.
761 https://doi.org/10.1155/2013/183041

762 Weiss, N., Miller, F., Cazaubon, S., Couraud, P.-O., 2009. The blood-brain barrier in brain
763 homeostasis and neurological diseases. Biochim. Biophys. Acta BBA - Biomembr., Apical
764 Junctional Complexes Part II 1788, 842–857. https://doi.org/10.1016/j.bbamem.2008.10.022

765 Werner, C., Reeker, W., Engelhard, K., Lu, H., Kochs, E., 1997. [Ketamine racemate and S-
766 (+)-ketamine. Cerebrovascular effects and neuroprotection following focal ischemia].
767 Anaesthesist 46 Suppl 1, S55-60

768 Xu, X., Yang, Y., Wang, R., Wang, Y., Ruan, Q., Lu, Y., 2015. Perinatal exposure to di-(2-
769 ethylhexyl) phthalate affects anxiety- and depression-like behaviors in mice. Chemosphere
770 124, 22–31. https://doi.org/10.1016/j.chemosphere.2014.10.056

771 You, M., Dong, J., Fu, Y., Cong, Z., Fu, H., Wei, L., Wang, Yi, Wang, Yuan, Chen, J., 2018.
772 Exposure to Di-(2-ethylhexyl) Phthalate During Perinatal Period Gender-Specifically Impairs
773 the Dendritic Growth of Pyramidal Neurons in Rat Offspring. Front. Neurosci. 12.
774 https://doi.org/10.3389/fnins.2018.00444

775

776

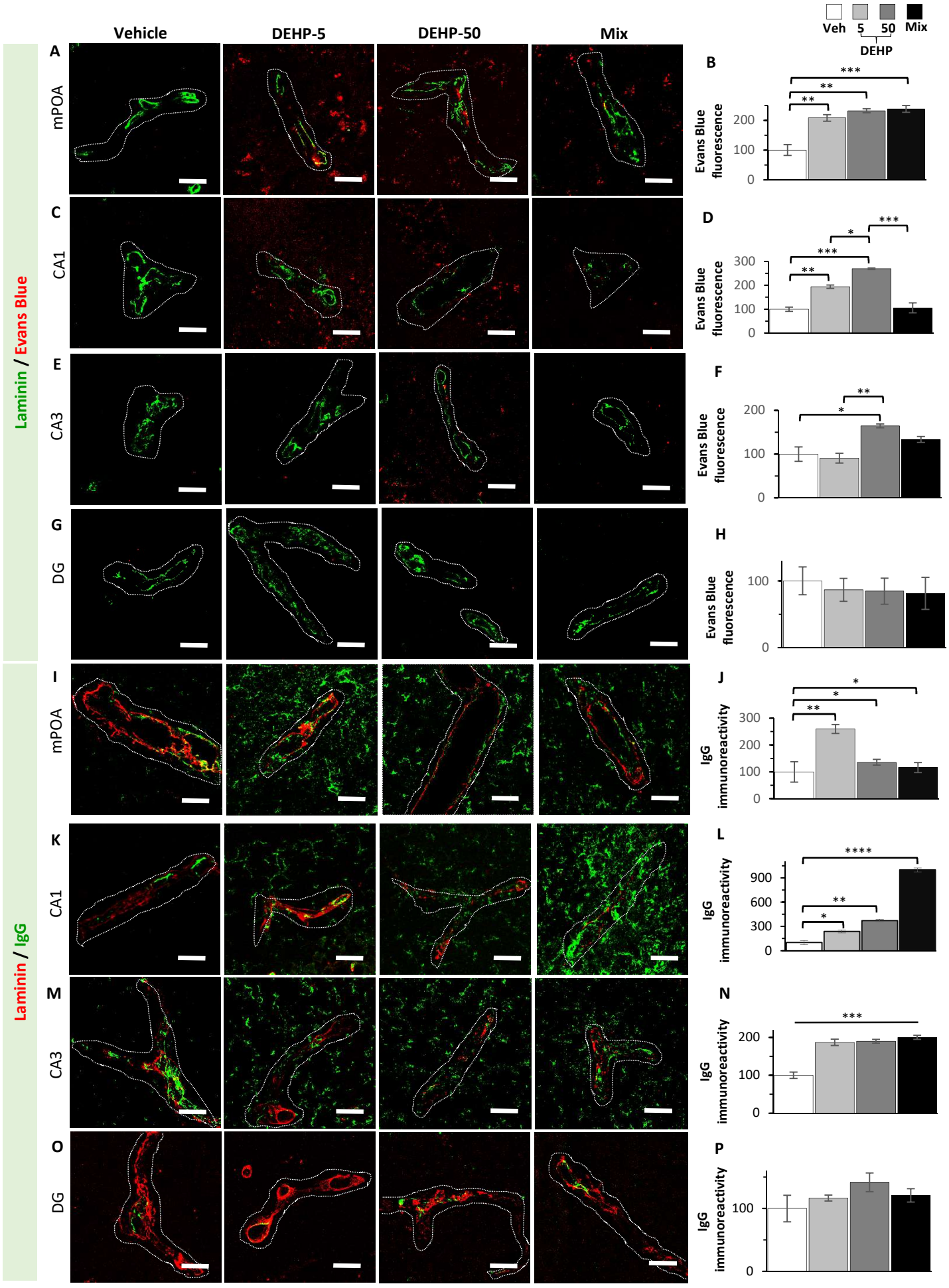
Vehicle
DEHP-5
DEHP-50
Mix
Veh
5
50
Mix
DEHP
Laminin / Evans Blue
Laminin / IgG
A
mPOA
B
Evans Blue fluorescence
C
CA1
D
E
CA3
F
G
DG
H
I
J
IgG immunoreactivity
K
L
M
N
O
P

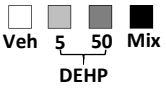


## mPOA

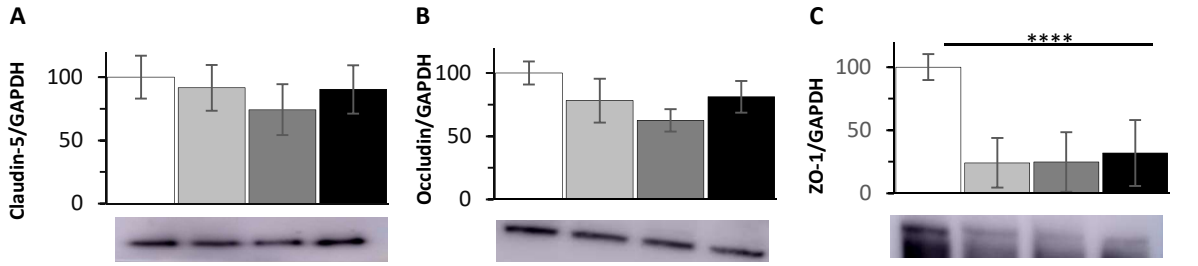


## Hippocampus

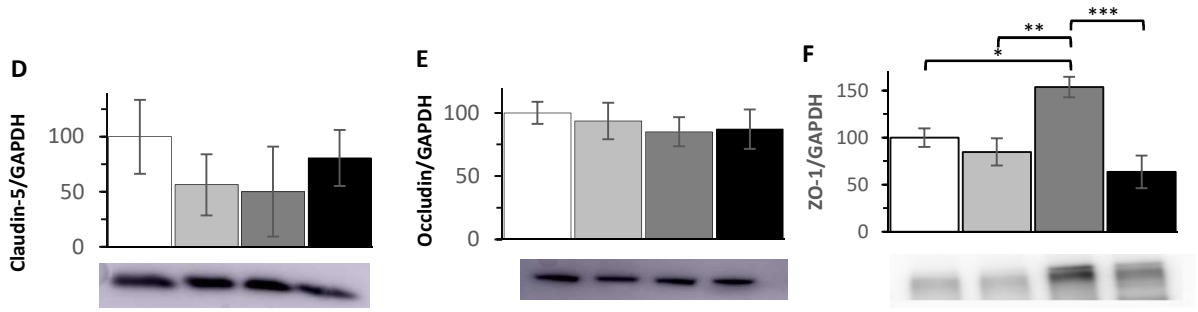

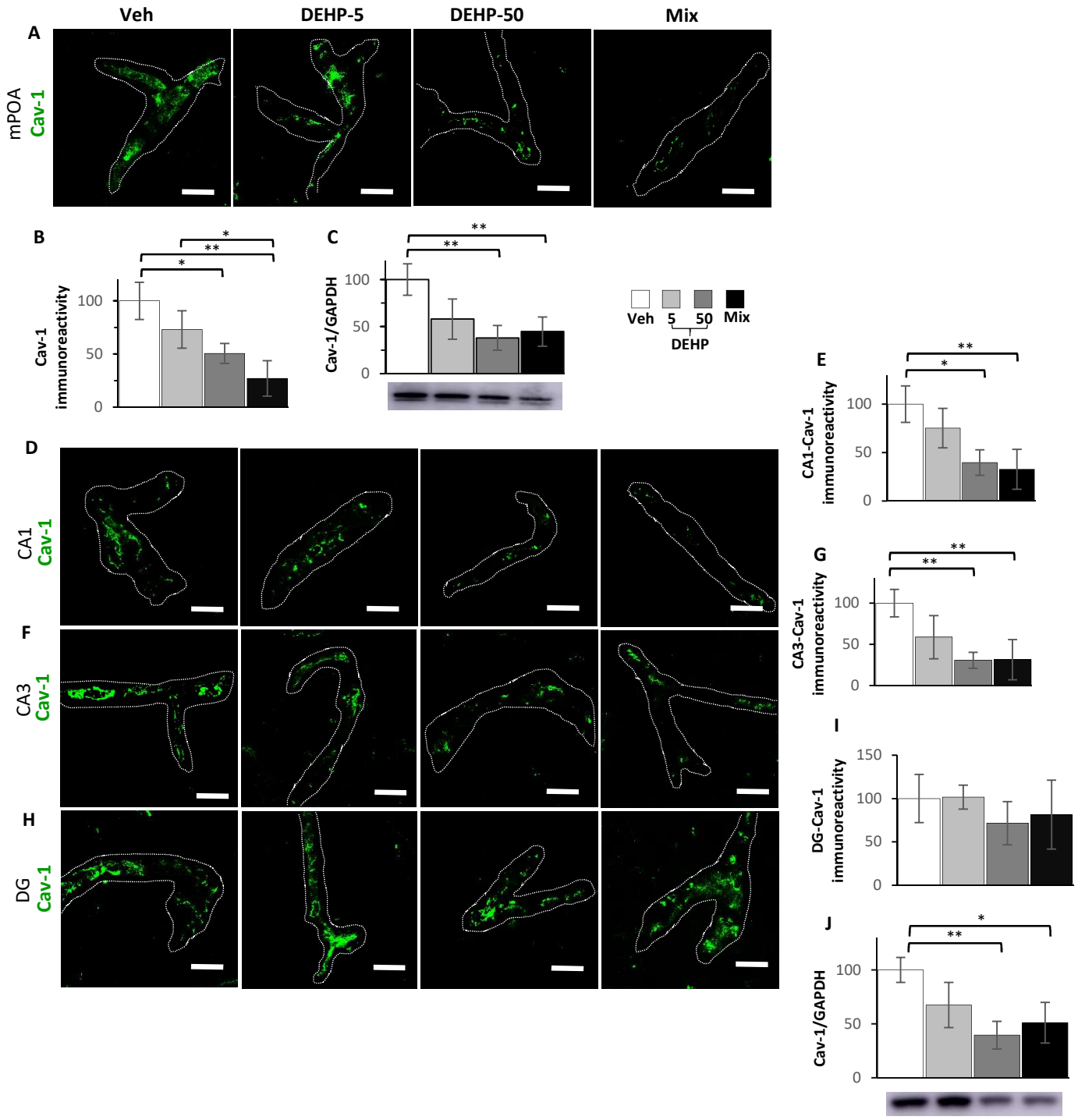
Veh
DEHP-5
DEHP-50
Mix
A
mPOA
Cav-1
B
Cav-1 immunoreactivity
100
50
0
*
**
*
C
Cav-1/GAPDH
100
50
0
**
**
Veh
5
50
Mix
DEHP
D
CA1
Cav-1
E
CA1-Cav-1 immunoreactivity
100
50
0
**
*
F
CA3
Cav-1
G
CA3-Cav-1 immunoreactivity
100
50
0
**
**
H
DG
Cav-1
I
DG-Cav-1 immunoreactivity
150
100
50
0
J
Cav-1/GAPDH
100
50
0
*
**

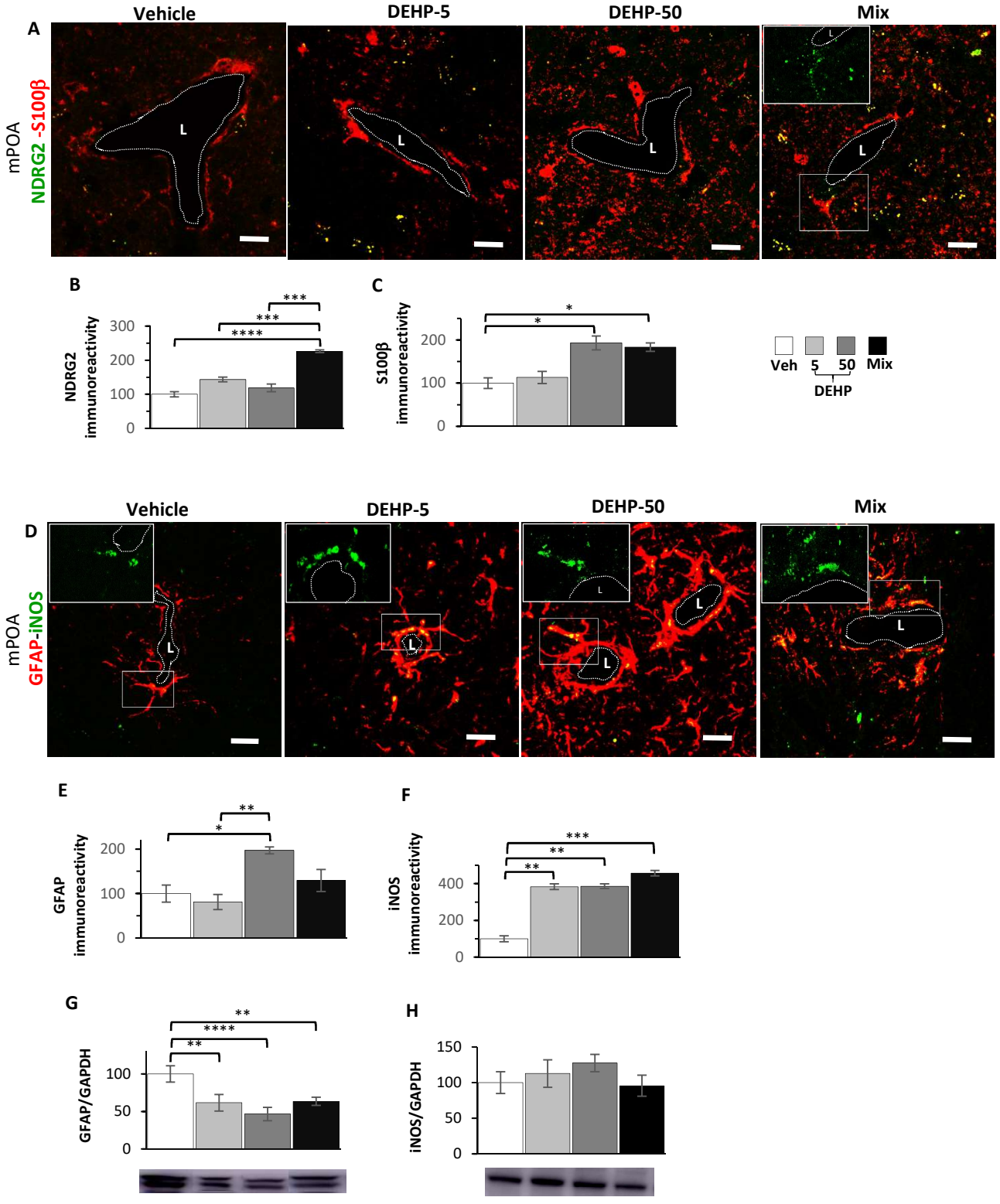
A
Vehicle
DEHP-5
DEHP-50
Mix
mPOA
NDRG2 -S100β
L
B
NDRG2 immunoreactivity
300
200
100
0
***
***
****
C
S100β immunoreactivity
200
100
0
*
*
Veh
5
50
Mix
DEHP
D
Vehicle
DEHP-5
DEHP-50
Mix
mPOA
GFAP-iNOS
E
GFAP immunoreactivity
200
100
0
**
*
F
iNOS immunoreactivity
400
200
0
***
**
**
G
GFAP/GAPDH
100
50
0
**
****
**
H
iNOS/GAPDH
150
100
50
0

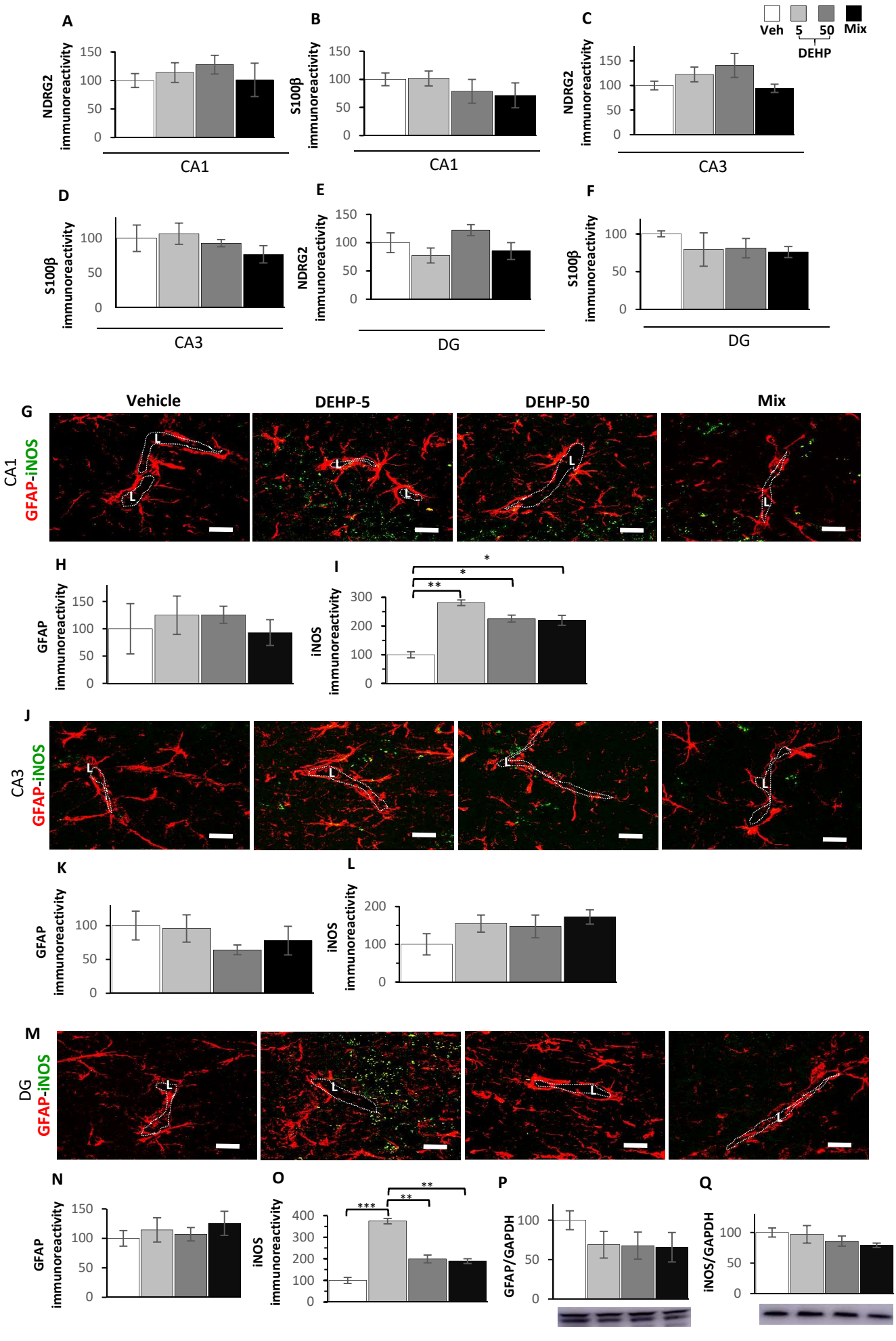
A
B
C
Veh
5
50
Mix
DEHP
NDRG2 immunoreactivity
S100β immunoreactivity
CA1
CA3
D
E
F
DG
G
Vehicle
DEHP-5
DEHP-50
Mix
CA1
GFAP-iNOS
H
I
GFAP immunoreactivity
iNOS immunoreactivity
J
CA3
K
L
M
DG
N
O
P
Q
GFAP/GAPDH
iNOS/GAPDH

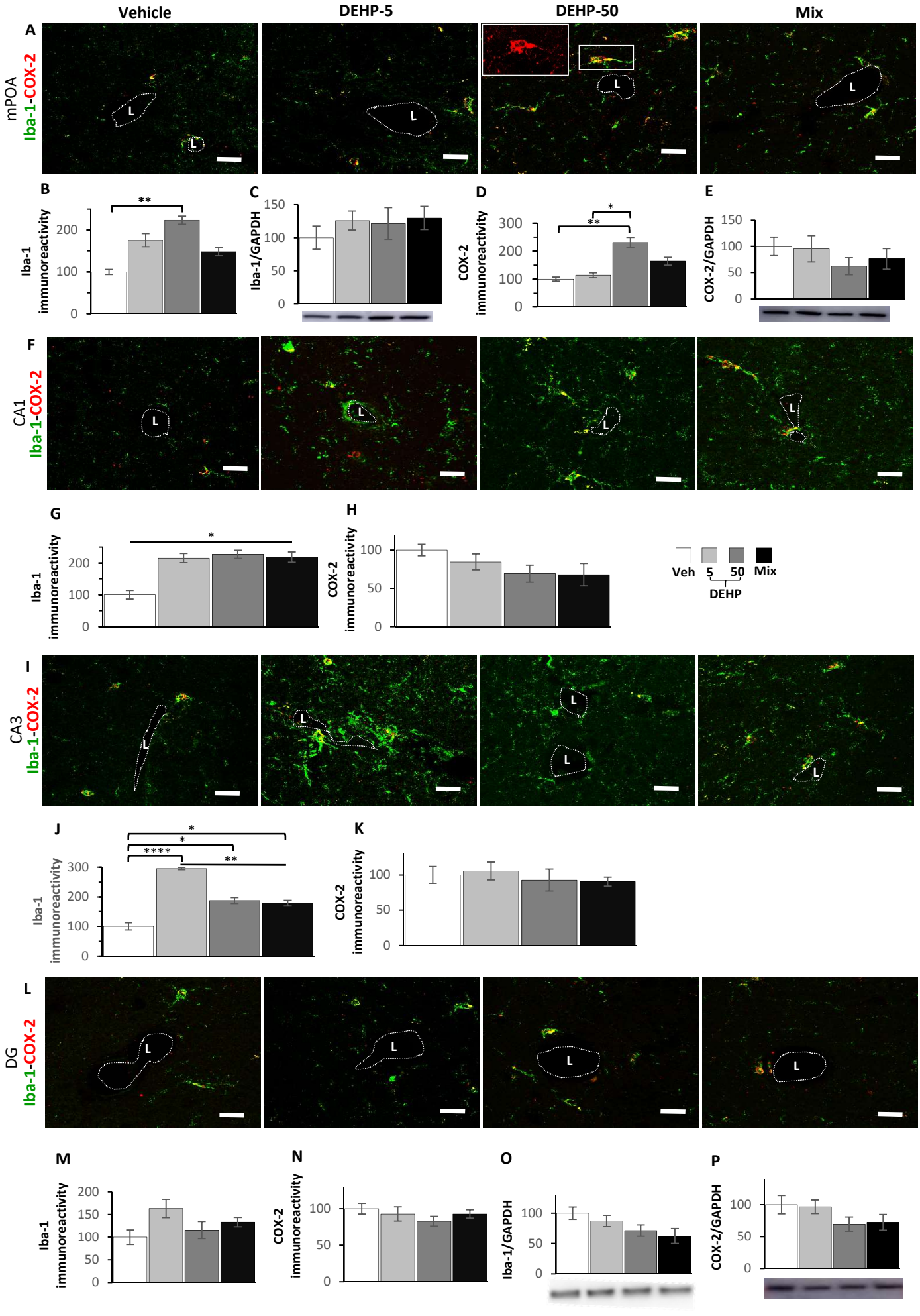
Vehicle
DEHP-5
DEHP-50
Mix
A
mPOA
Iba-1-COX-2
L
B
Iba-1 immunoreactivity
C
Iba-1/GAPDH
D
COX-2 immunoreactivity
E
COX-2/GAPDH
F
CA1
G
H
Veh
5
50
Mix
DEHP
I
CA3
J
K
L
DG
M
N
O
P

# Figure legends

**Figure 1. Exposure to DEHP alone or in a phthalate mixture increased BBB permeability to Evans blue dye and endogenous IgG.**

The permeability of BBB was analyzed using Evans blue dye (n=3 per group, A to H) and immunolabeled endogenous IgG (n=5 per group, I to P) in the hypothalamic medial preoptic area (mPOA) and hippocampal CA1, CA3 and DG. Images were selected from brain sections containing the sub-regions of interest in adult male mice orally exposed to vehicle (Veh; first column), DEHP at 5 µg/kg/d (DEHP-5; second column), DEHP at 50 µg/kg/d (DEHP-50; third column) and a phthalate mixture (Mix; fourth column). (A-H) Representative images and corresponding quantitative analysis of the six to eight serial sections for each brain examined of the mPOA (A, B), CA1 (C, D), CA3 (E, F) and DG (G, H) for Evans blue dye tracer (red), capillaries were labeled with anti-laminin (green). (I-P) Representative images and corresponding quantitative analysis of the six to eight serial sections for each brain examined of the mPOA (I, J), CA1 (K, L), CA3 (M, N) and DG (O, P) of endogenous circulating IgG (green), capillaries were labeled with anti-laminin (red).

$*p < 0.05$; $**p < 0.01$; $***p < 0.001$; $****p < 0.0001$ compared to vehicle-treated mice compared to the vehicle group. All data are expressed as mean percentages ± S.E.M of vehicle (100%).

The pictures presented are the projection of 3 successive optical sections (1 µm) into one image.

Scale bar: 10 µm. The dotted lines delimit the outer contour of the capillaries. The quantifications of fluorescence density were measured over the entire surface of the images.

**Figure 2. Exposure to DEHP alone or in a phthalate mixture affected endothelial tight junction protein ZO-1 levels but not claudin-5 and occludin protein levels.**

Western blot analysis (n = 6 per treatment group) of tight junction proteins performed on microvessel-enriched fractions from hypothalamus (A-C) and hippocampus (D-F) of mice exposed to the Vehicle (Veh), DEHP at 5 µg/kg/d (DEHP-5), DEHP at 50 µg/kg/d (DEHP-50) or the phthalate mixture (Mix). All data are expressed as mean percentages ± S.E.M of vehicle (100%). *$p < 0.05$; **$p < 0.01$; ***$p < 0.001$; ****$p < 0.0001$ compared to the vehicle group. Data were normalized to GAPDH level.

**Figure 3. Exposure to DEHP alone or in a phthalate mixture decreased protein levels of the caveolae-associated membrane protein Cav-1.**

Images were selected from brain sections containing the sub-regions of interest in adult male mice orally exposed to vehicle (Veh; first column), DEHP at 5 µg/kg/d (DEHP-5; second column), DEHP at 50 µg/kg/d (DEHP-50; third column) and a phthalates mixture (Mix; fourth column). (A, B) Representative images of immunodetection of Cav-1 in the mPOA (A) and the corresponding quantitative analysis of the Cav-1 immunoreactivity density (B) of the six to eight serial sections for each brain examined (n = 5 per treatment group). Values represent mean percentages ± S.E.M of vehicle (100%). *$p < 0.05$; **$p < 0.01$ compared to the vehicle group. (C) Western blot analysis of Cav-1 performed on microvessel-enriched fractions. *$p < 0.05$; **$p < 0.01$ compared to the vehicle group (n = 6 per treatment group). Data were normalized to GAPDH levels.

(D-I) Representative images of immunodetection of Cav-1 in the hippocampus (D: CA1; F: CA3; H: DG) and the corresponding quantitative analysis of the Cav-1 immunoreactivity density (E: CA1; G: CA3; I: DG) of the six to eight serial sections for each brain examined (n=5 per group). *$p < 0.05$; **$p < 0.01$compared to the vehicle group. (J) Western blot analysis of Cav-1 performed on microvessel-enriched fractions from hippocampus. *$p < 0.05$; **$p < 0.01$ compared to the vehicle group (n = 6 per treatment group). Data were normalized to GAPDH level.

Scale bar: 10 µm. The dotted lines delimit the outer contour of the capillaries. The quantifications of fluorescence density were measured over the entire surface of the images. All values represent mean percentages ± S.E.M of vehicle (100%).

**Figure 4. Exposure to DEHP alone or in a phthalate mixture induced astrocyte activation and iNOS expression in the medial preoptic area (mPOA).**

(A-C) Representative images (A) and corresponding quantitative analysis (B, C) of the six to eight serial sections for each brain examined of the co-immunolabeling of NDRG2 (green, insert) and S100ß (red) in the mPOA of mice exposed to the vehicle (Veh), DEHP at 5 µg/kg/d (DEHP-5), DEHP at 50 µg/kg/d, or phthalate mixture (Mix) (n = 5 per treatment group). (D-F) Representative images (D) and corresponding quantitative analysis (E, F) of the six to eight serial sections for each brain examined of the co-immunolabeling of iNOS (green, inserts) and GFAP (red) in the mPOA (n=5 per group). *$p < 0.05$; ***$p < 0.001$; ****$p < 0.0001$ compared to the vehicle group.

(G, H) Western blot analysis (n = 6 per treatment group) of GFAP (G) and iNOS (H) performed on microvessel-enriched fractions from the hypothalamus. *$p < 0.05$; **$p< 0.01$; ***$p < 0.001$; ****$p < 0.0001$ compared to the vehicle group (n=6 per group). Data were normalized to GAPDH level.

Scale bar: 10 µm. L: Lumen delimited by the dotted lines. The quantifications of fluorescence density were measured over the entire surface of the images. All values represent mean percentages ± S.E.M of vehicle (100%).

**Figure 5. Exposure to DEHP alone or in a phthalate mixture had no effect on astrocyte activation in the hippocampus but induced iNOS expression in the CA1 and DG.**

(A-F) Quantitative analysis of the immunoreactivity of NDRG2 and S100ß in the hippocampus (A, B: CA1; C D: CA3; E, F: DG) of the six to eight serial sections for brain collected from mice exposed to the vehicle (Veh), DEHP at 5 µg/kg/d (DEHP-5), DEHP at 50 µg/kg/d, or phthalate mixture (Mix) (n = 5 per treatment group). No significant difference was measured compared to vehicle-treated controls.

(G-O) Representative images of co-immunodetection of GFAP (red) and iNOS (green) in the hippocampus (G: CA1; J: CA3; M: DG) and their corresponding quantitative analysis of the immunoreactivity density (H, I: CA1; K, L: CA3; N, O: DG) of the six to eight serial sections for each brain examined (n=5 per group). *$p < 0.05$; **$p < 0.01$; ***$p < 0.001$ compared to vehicle-treated controls.

(P, Q) Western blot analysis (n=6 per group) of GFAP (P) and iNOS (Q) performed on microvessel-enriched fractions from hippocampus. Data were normalized to GAPDH level. No significant difference was measured compared to vehicle-treated controls.

Scale bar: 10 µm. L: Lumen delimited by the dotted lines. The quantifications of fluorescence density were measured over the entire surface of the images. All values represent mean percentages ± S.E.M of vehicle (100%).

**Figure 6. Exposure to DEHP alone or in a phthalate mixture induced microglia activation in the testosterone-sensitive cerebral regions, the medial preoptic area (mPOA) and the hippocampus, and increased COX-2 expression in the mPOA.**

(A, B, D) Representative images (A) and corresponding quantitative analysis (B, D) of the six to eight serial sections for each brain examined of the co-immunolabeling of Iba-1 (green) and COX-2(red, insert) in the mPOA of mice exposed to the vehicle (Veh), DEHP at 5 µg/kg/d (DEHP-5), DEHP at 50 µg/kg/d, or phthalate mixture (Mix) (n = 5 per treatment group). *$p < 0.05$; **$p < 0.01$ compared to the vehicle group. (C, E) Western blot analysis (n = 6 per treatment group) of Iba-1 (C) and COX-2 (E) performed on microvessel-enriched fractions from

hypothalamus. *$p < 0.05$; **$p < 0.01$ compared to the vehicle group. Data were normalized to GAPDH level.

(F-N) Representative images of co-immunodetection of Iba-1 (green) and COX-2 (red) in the hippocampus (F: CA1; I: CA3; L: DG) and their corresponding quantitative analysis of the immunoreactivity density (G, H: CA1; J, K: CA3; M, N: DG) of the six to eight serial sections for each brain examined (n = 5 per treatment group). *$p < 0.05$; **$p < 0.01$; ***$p < 0.001$; ****$p < 0.0001$ compared to vehicle-treated controls. (O, P) Western blot analysis (n = 6 per treatment group) of Iba-1 (O) and COX-2 (P) performed on microvessel-enriched fractions from hippocampus. Data were normalized to GAPDH level. No significant difference was measured compared to vehicle-treated controls.

Scale bar: 10 µm. L: Lumen delimited by the dotted lines. The quantifications of fluorescence density were measured over the entire surface of the images. All values represent mean percentages ± S.E.M of the vehicle (100%).

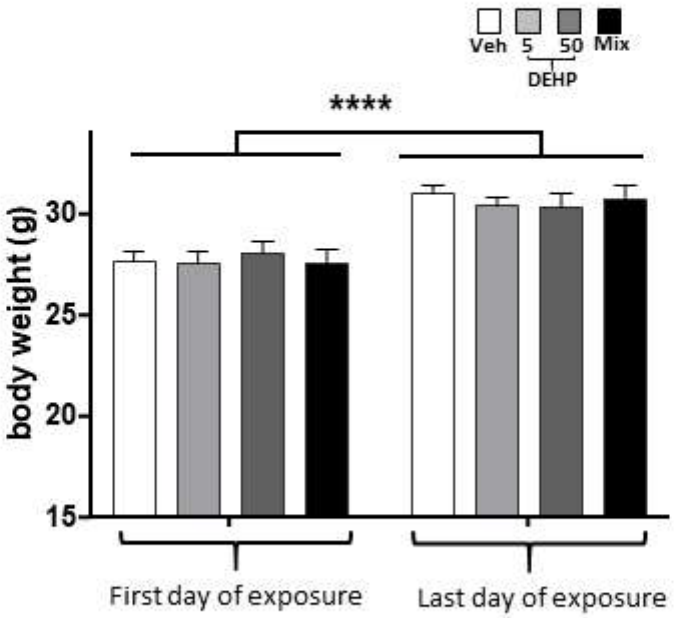
Veh
5
50
Mix
DEHP
****
body weight (g)
30
25
20
15
First day of exposure
Last day of exposure

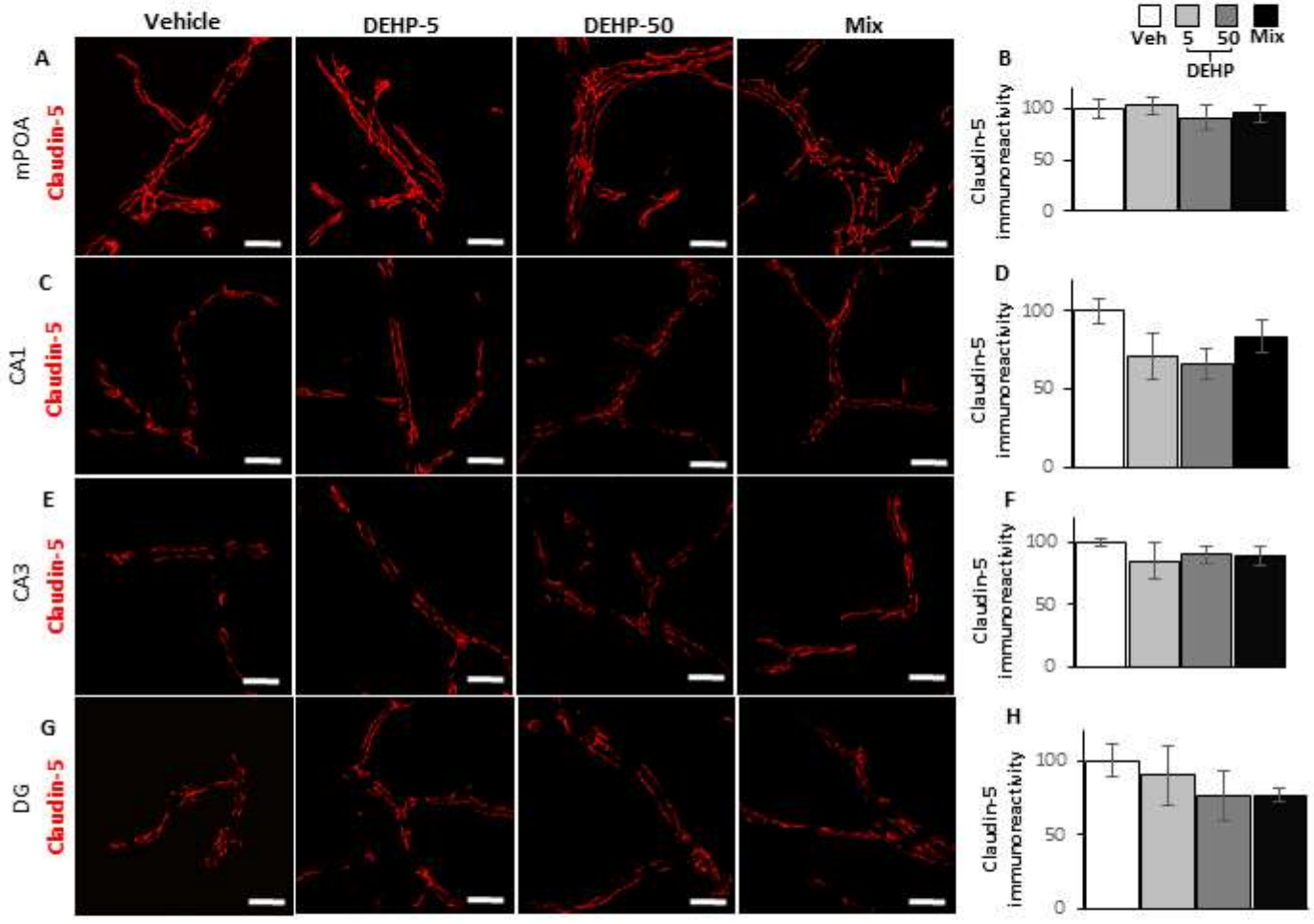
Vehicle
DEHP-5
DEHP-50
Mix
A
mPOA
Claudin-5
B
Veh
5
50
Mix
DEHP
Claudin-5 immunoreactivity
100
50
0
C
CA1
Claudin-5
D
Claudin-5 immunoreactivity
100
50
0
E
CA3
Claudin-5
F
Claudin-5 immunoreactivity
100
50
0
G
DG
Claudin-5
H
Claudin-5 immunoreactivity
100
50
0

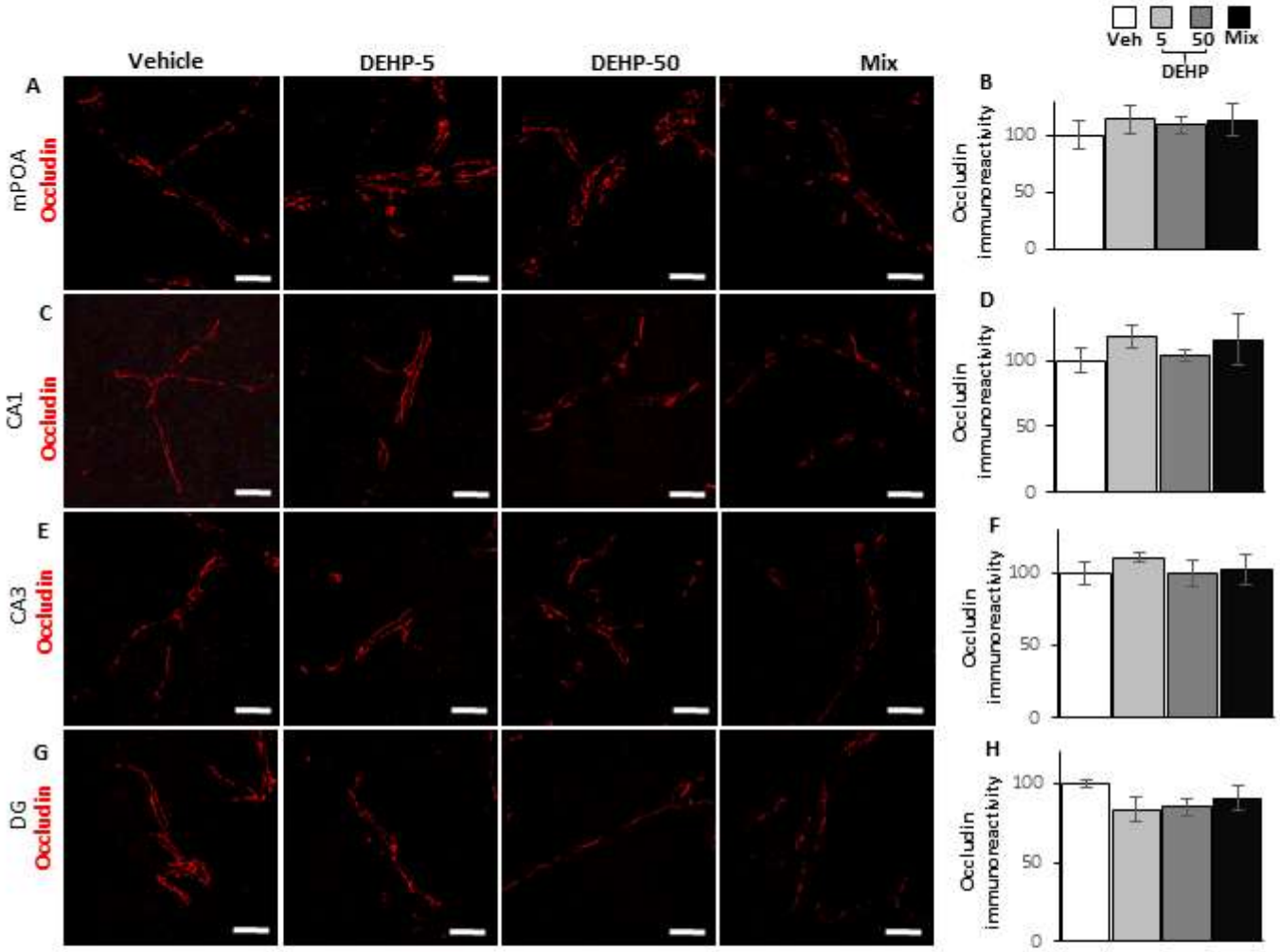
Vehicle
DEHP-5
DEHP-50
Mix
A
mPOA
Occludin
B
C
CA1
D
E
CA3
F
G
DG
H
Veh
5
50
Mix
DEHP
Occludin immunoreactivity
100
50
0

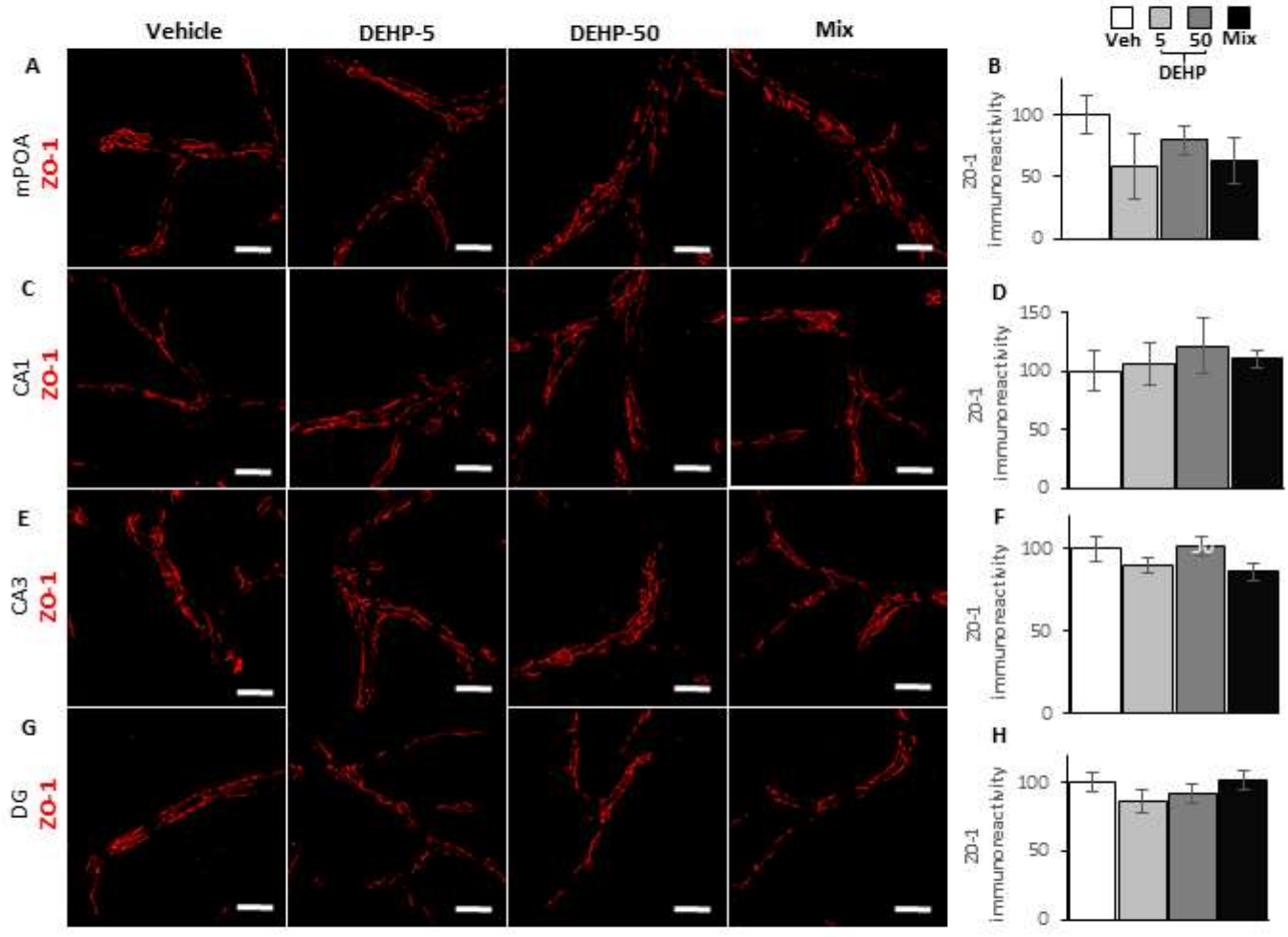
Vehicle
DEHP-5
DEHP-50
Mix
A
mPOA
ZO-1
B
Veh
5
50
Mix
DEHP
ZO-1 immunoreactivity
100
50
0
C
CA1
ZO-1
D
150
100
50
0
E
CA3
ZO-1
F
G
DG
ZO-1
H

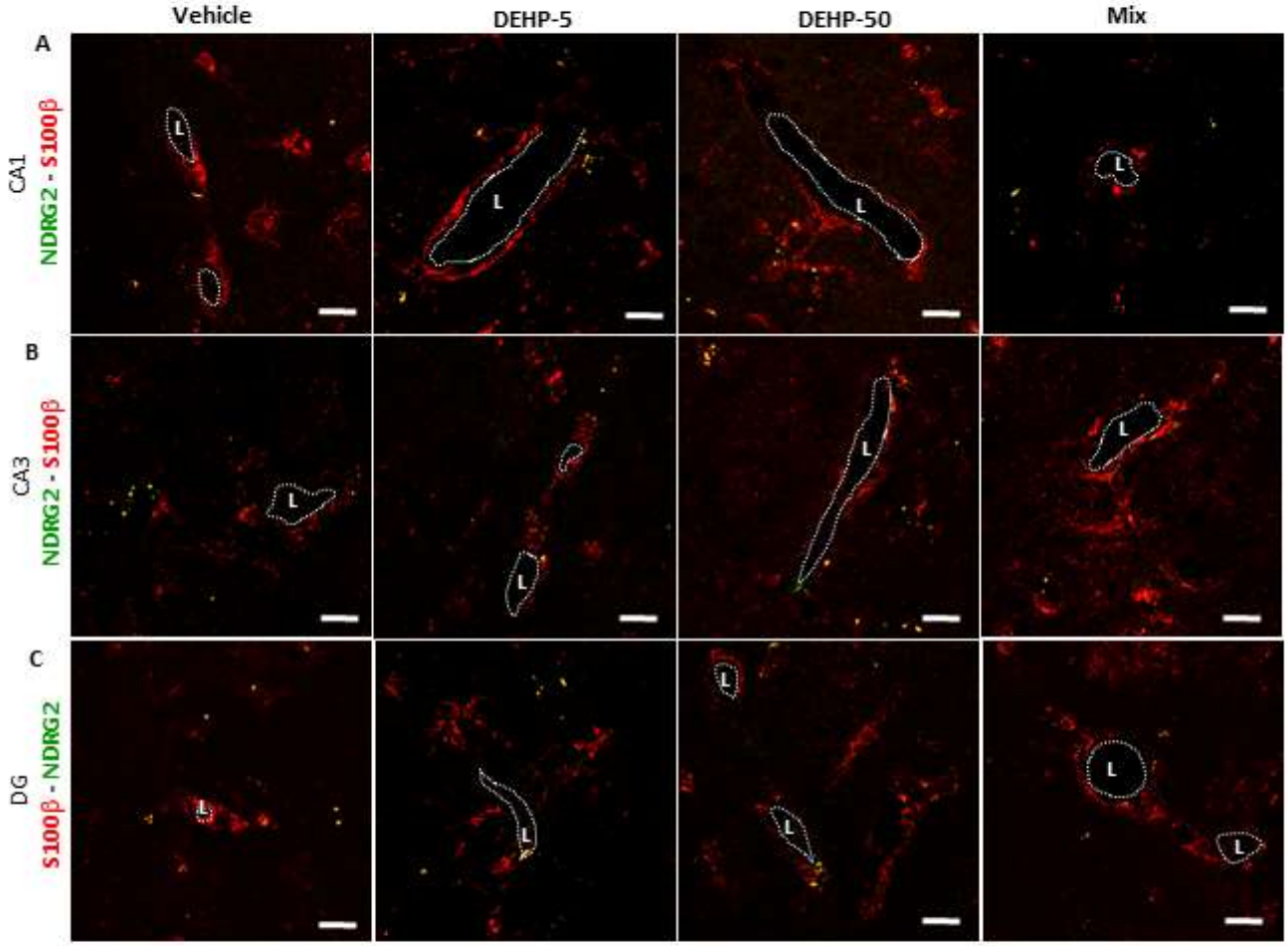
Vehicle
DEHP-5
DEHP-50
Mix
A
CA1
NDRG2 - S100β
B
CA3
NDRG2 - S100β
C
DG
S100β - NDRG2
L

**Figure S1. Exposure to DEHP alone or in a phthalate mixture did not affect the body weight of treated mice.**

The body weight of male mice exposed to the vehicle (Veh), DEHP at 5 µg/kg/d (DEHP-5), DEHP at 50 µg/kg/d (DEHP-50), or a phthalate mixture (Mix), is reported for the first and last days of exposure. The values represent body weight means (g) ± S.E.M (n = 12 per treatment group). There was an effect of time ($F_{(1, 88)} = 48.8$, $p < 0{,}0001$) but not of treatment ($F_{(3, 88)} = 0{,}1063$, $p = 0.9562$).

**Figure S2. Exposure to DEHP alone or in a phthalate mixture did not affect claudin-5 immunoreactivity.**

(A, B) Representative images of immunodetection of claudin-5 in the mPOA of mice exposed to the vehicle (Veh), DEHP at 5 µg/kg/d (DEHP-5), DEHP at 50 µg/kg/d (DEHP-50), or phthalate mixture (Mix) (A) and their corresponding quantitative analysis of the immunoreactivity density (B) of the six to eight serial sections for each brain examined (n = 5 per treatment group). No significant difference was measured compared to vehicle-treated controls. (C-H) Representative images of immunodetection of claudin-5 (C: CA1; E: CA3; G: DG) and the corresponding quantitative analysis of the immunoreactivity density (D: CA1; F: CA3; H: DG) of the six to eight serial sections for each brain examined (n=5 per group). No significant difference was measured compared to vehicle-treated controls.

Scale bar: 10 µm. The quantifications of fluorescence density were measured over the entire surface of the images and the values represent mean percentages ± S.E.M of vehicle (100%).

**Figure S3. Exposure to DEHP alone or in a phthalate mixture did not affect occludin immunoreactivity.**

(A, B) Representative images of immunodetection of occludin in the mPOA of mice exposed to the vehicle (Veh), DEHP at 5 µg/kg/d (DEHP-5), DEHP at 50 µg/kg/d (DEHP-50), or phthalate mixture (Mix) (A) and their corresponding quantitative analysis of the immunoreactivity density (B) of the six to eight serial sections for each brain examined (n=5 per group). No significant difference was measured compared to vehicle-treated controls. (C-H) Representative images of immunodetection of occludin in the hippocampus (C: CA1; E: CA3; G: DG) and the corresponding quantitative analysis of the immunoreactivity density (D: CA1; F: CA3; H: DG) of the six to eight serial sections for each brain examined (n = 5 per treatment group). No significant difference was measured compared to vehicle-treated controls.

Scale bar: 10 µm. The quantifications of fluorescence density were measured over the entire surface of the images and the values represent mean percentages ± S.E.M of vehicle (100%).

**Figure S4. Exposure to DEHP alone or in a phthalate mixture did not affect ZO-1 immunoreactivity.**

(A, B) Representative images of immunodetection of ZO-1 in the mPOA of mice exposed to the vehicle (Veh), DEHP at 5 µg/kg/d (DEHP-5), DEHP at 50 µg/kg/d (DEHP-50), or a phthalate mixture (Mix) (A) and their corresponding quantitative analysis of the immunoreactivity density (B) of the six to eight serial sections for each brain examined (n=5 per group). No significant difference was measured compared to vehicle-treated controls. (C-H) Representative images of immunodetection of ZO-1 in the hippocampus (C: CA1; E: CA3; G: DG) and the corresponding quantitative analysis of the immunoreactivity density (D: CA1; F: CA3; H: DG) of the six to eight

serial sections for each brain examined (n = 5 per treatment group). No significant difference was measured compared to vehicle-treated controls.

Scale bar: 10 µm. The quantifications of fluorescence density were measured over the entire surface of the images and the values represent mean percentages ± S.E.M of vehicle (100%).

**Figure S5. Exposure to DEHP alone or in a phthalate mixture did not affect NDRG2 and S100ß immunoreactivity in the hippocampus.**

Representative images of co-immunodetection of NDRG2 (green) and S100ß (red) in the hippocampal CA1 (A), CA3 (B) and DG (C) of mice exposed to the vehicle (Veh), DEHP at 5 µg/kg/d (DEHP-5), DEHP at 50 µg/kg/d (DEHP-50), or phthalate mixture (Mix).

Scale bar: 10 µm. L: Lumen delimited by the dotted lines.

**Table 1: List of primary antibodies**

| Antibody | Host | Manufacturer | Catalog no | Application | Working dilution |
|---|---|---|---|---|---|
| NDRG2 | Rabbit | Cell Signaling Technology | 5667S | IHC | 1/400 |
| S100β | Mouse | Sigma-Aldrich | s2532 | IHC | 1/1000 |
| COX-2 | Goat | Santa Cruz | Sc-1747 | IHC - WB | 1/200 |
| Iba-1 | Rabbit | WAKO | 016-20001 | WB | 1/500 |
| Iba-1 | Rabbit | Biocare Medical | CP-290 | IHC | 1/300 |
| ZO-1 | Rabbit | Invitrogen | 61-7300 | IHC - WB | 1/125 - 1/500 |
| Claudin-5 | Rabbit | Invitrogen | 34-1600 | IHC - WB | 1/500 |
| Cav-1 | Mouse | Biosciences | 610407 | IHC | 1/200 |
| Cav-1 | Mouse | Santa Cruz | sc-53564 | WB | 1/200 |
| iNOS | Mouse | Santa Cruz | sc-7271 | WB | 1/200 |
| iNOS | Mouse | Sigma-Aldrich | n9657 | IHC | 1/1000 |
| GFAP | Mouse | Sigma-Aldrich | G3893 | WB | 1/500 |
| GFAP | Rabbit | DAKO | Z0334 | IHC | 1/500 |
| Laminin | Rabbit | Sigma-Aldrich | L9393 | IHC - WB | 1/200 - 1/100 |
| Occludin | Rabbit | Invitrogen | 40-4700 | IHC - WB | 1/500 - 1/250 |
| GAPDH | Mouse | Santa Cruz | sc-32233 | WB | 1/10000 |

IHC: Immunohistochistry; WB: Western blotting

**Table 2: Synthesis of the effects of an oral exposure during adulthood to low doses of DEHP alone or in phthalate mixture in male mice on BBB integrity and associated inflammation in the hypothalamus and hippocampus**

| | | | Immunohistochemitry analysis | | | | Western blot analysis | |
|---|---|---|---|---|---|---|---|---|
| | | | **mPOA** | **CA1** | **CA3** | **DG** | **Hypothalamus** | **Hippocampus** |
| **BBB integrity** | **Permeability** | *Evans blue extravasation* | increased: DEHP-5, DEHP-50 and Mix | increased: DEHP-5 and DEHP-50 | increased: DEHP-50 | not affected | n.d. | n.d. |
| | | *Endogenous IgG extravasation* | increased: DEHP-5, DEHP-50 and Mix | increased: DEHP-5, DEHP-50 and Mix | increased: DEHP-5, DEHP-50 and Mix | not affected | n.d. | n.d. |
| | **Endothelial tight junctions** | *Claudin-5* | not affected | not affected | not affected | not affected | not affected | not affected |
| | | *Occludin* | not affected | not affected | not affected | not affected | not affected | not affected |
| | | *ZO-1* | not affected | not affected | not affected | not affected | decreased: DEHP-5, DEHP-50 and Mix | increased: DEHP-50 |
| | **Trans-endothelial vesicular transport** | *Cav-1* | decreased: DEHP-50 and Mix | decreased: DEHP-50 and Mix | decreased: DEHP-50 and Mix | not affected | decreased: DEHP-50 and Mix | decreased: DEHP-50 and Mix |
| **Inflammation** | **Astrocyte activation** | *NDRG2* | increased: Mix | not affected | not affected | not affected | n.d. | n.d. |
| | | *S100 β* | increased: DEHP-50 and Mix | not affected | not affected | not affected | n.d. | n.d. |
| | | *GFAP* | increased: DEHP-50 | not affected | not affected | not affected | decreased: DEHP-5, DEHP-50 and Mix | not affected |
| | **Microglia activation** | *Iba-1* | increased: DEHP-50 | increased: DEHP-5, DEHP-50 and Mix | increased: DEHP-5, DEHP-50 and Mix | not affected | not affected | not affected |
| | **Inflammatory molecules** | *iNOS* | increased: DEHP-5, DEHP-50 and Mix | increased: DEHP-5, DEHP-50 and Mix | not affected | increased: DEHP-5 | not affected | not affected |
| | | *COX-2* | increased: DEHP-50 | not affected | not affected | not affected | not affected | not affected |

n.d.: not determined; DEHP-5: DEHP at 5µg/kg/d; DEHP-50: DEHP at 50 µg/kg/d; Mix: phthalate mixture